The Dissertation Committee for Rachael Madlyn Rossi Certifies that this is the approved version of the following dissertation:

Role of cardiolipin in *Shigella flexneri* pathogenesis

Committee:

Shelley M. Payne, Supervisor

Marvin Whiteley

Bryan Davies

Theresa J. O'Halloran

Somshuvra Mukhopadhyay

Role of cardiolipin in *Shigella flexneri* pathogenesis

by

Rachael Madlyn Rossi

Dissertation

Presented to the Faculty of the Graduate School of

The University of Texas at Austin

in Partial Fulfillment

of the Requirements

for the Degree of

Doctor of Philosophy

The University of Texas at Austin

December 2017

Dedication

This work is dedicated to my selfless parents.

Their wisdom and guidance has instilled in me the value of persistence, power of humility and the importance for a lifetime full of learning. Without their unconditional love and encouragement none of my success would be possible.

Acknowledgements

I am grateful for the supportive and collaborative learning environment at The University of Texas at Austin, and the friendships I have made during my doctoral work. I would first like to thank my dissertation advisor, Shelley Payne, for her guidance, mentorship and support during the process of earning my doctorate.

I am grateful for her commitment to developing independent scientists, and for her expertise and advice that taught me to push my science further. I would also like to thank the other members of my dissertation committee for their insight and feedback that contributed greatly to my dissertation research.

I would like to thank my colleagues in the Payne Lab, as being a member of this lab has been a very special and rewarding experience. They have made coming to work more enjoyable and I am grateful to have learned and developed my research skill from so many talented scientists. Specifically to Alex Mey and Liz Wyckoff for their critical feedback, and to Carolyn Fisher for her technical and moral support.

I would also like to thank Ben Koestler for his help with tissue culture techniques, Minhye Shin for her help with protein purification, Emily Nolwicki for her help with lipid techniques, and Hervé Agaisse and Laurn Yum (University of Virginia) for their help with microscopy techniques.

I would especially like to thank Heidi Butz and Charlie Zozgas for their friendship throughout this process; their companionship and laughter will be missed dearly.

I am grateful for my supportive family and friends that took the time to visit me during my time in Texas. Specifically, I would like to thank my parents for their lifelong encouragement and support that has allowed me to pursue my dreams.

Lastly, I would like to give a very special thank you to Ryan Linderman for his inspiration, despite being far away, and patience. I am thankful for his shared passion for STEM and dedication to learning. I could not have done this without him.

Role of cardiolipin in *Shigella flexneri* pathogenesis

Rachael Madlyn Rossi, Ph.D.

The University of Texas at Austin, 2017

Supervisor: Shelley M. Payne

Shigella flexneri causes bacterial dysentery in humans by invading colonic epithelial cells, and then replicating and moving within the host cell cytoplasm to spread intercellularly to neighboring epithelial cells. Analysis of *S. flexneri* phospholipids revealed that cardiolipin, a large anionic phospholipid that localizes to the inner leaflet at the poles of Gram-negative bacterial membrane, makes up approximately 7% of *S. flexneri*'s total phospholipids and is found in equal proportions between the inner and outer membrane. To characterize the mechanisms *S. flexneri* uses to synthesize and transport cardiolipin, a series of mutants were construed that disrupted one of the three putative cardiolipin synthases, *clsA*, *clsB*, and *clsC*, or transporter, *pbgA*. It was determined that ClsA is the major cardiolipin synthase of *S. flexneri* and the level of phosphatidylglycerol increases in both the inner and outer membrane in the absence of cardiolipin. In addition, PbgA transports cardiolipin and phosphatidylglycerol to the *S. flexneri* outer membrane, but has no effect on the inner membrane phospholipid composition. Both the *clsA* and *pbgA* mutants were unable to form wild type plaques in cultured epithelial cells, and time-lapse microscopy revealed that the *clsA* mutant was less motile intracellularly and unable to divide during intracellular growth, while the

pbgA mutant grew normally but was non-motile. This suggests inner membrane cardiolipin is required for cell division and outer membrane anionic phospholipids are required for motility. Unipolar localization of *S. flexneri* virulence protein IcsA, a member of the auto-transporter protein family, provides the mechanism for intracellular mobility through the polymerization of host actin. Analysis of IcsA localization on the surface of the *clsA* and *pbgA* mutants revealed reduced and pinpoint (respectively) levels of polar localized IcsA; however, both mutants displayed wild type levels of outer membrane IcsA, and surface exposed IcsA passenger domain. Protein-lipid co-sedimentation assays revealed a direct interaction of the polar targeting region in the passenger domain of IcsA with cardiolipin, and to a lesser extent with phosphatidylglycerol. We propose a novel model for IcsA polar localization directed by outer membrane anionic phospholipids, where outer membrane cardiolipin directs IcsA insertion and subsequent auto-transport at the bacterial pole.

Table of Contents

List of Tables

List of Figures

I. INTRODUCTION

1. Global burden of *Shigella* species

Shigella species are the causative agent for shigellosis, a form of bacterial dysentery, in humans (Musher & Musher, 2004). Shigellosis is highly contagious, and it is estimated that as few as 10 bacterial cells are required to initiate infection, which typically results from the consumption of fecal contaminated food or water sources (DuPont *et al*., 1989). The disease symptoms, include painful abdominal craping, fever, bloody diarrhea, and in some more serious cases arthritis, blood stream infections, seizures, and hemolytic-uremic syndrome, are the results of damage to the colonic epithelial layer by *Shigella* and subsequent inflammatory immune response of the host. People who are immune compromised, children under the age of 5, and the elderly are at risk for a more severe illness and death (Kotloff *et al*., 2013).

Each year, there are hundreds of millions of cases of shigellosis, with death rates as high as 15% in some countries (Bardhan *et al*., 2010). Most deaths resulting from shigellosis are among children under the age of five (Ashkenazi *et al*., 2003). Shigellosis rates are highest in developing countries with poor sanitation, affecting mostly children and the urban poor (Thapar & Sanderson, 2004). In developed countries, shigellosis incidence rates are lower; however, where there is overcrowding or close contact, such as day-care centers, prisons, and military barracks, shigellosis spreads rapidly. Programs aimed at improving water and sanitation systems have been successful at reducing shigellosis outbreaks in both developing and developed countries (Thompson *et al*., 2015).

Shigellosis symptoms begin 24-48 hours after infection, and usually last about 5-7 days (Schroeder & Hilbi, 2008). In most cases, symptoms resolve on their own; however, in more severe cases, antibiotics are necessary to reduce the duration of the disease and to clear the disease symptoms. The increased frequency of antimicrobial resistance among many *Shigella* species complicates shigellosis treatment. In 2013, the CDC declared antibiotic-resistant *Shigella* as an urgent threat to the United States and invoked the World Health Organization to launch global vaccine development programs to prevent *Shigella* outbreaks (Vohra & Blakely, 2013). Most recently, in 2017, the World Health Organization classified fluoroquinolone-resistant *Shigella* species a global priority pathogen for research and development of new antibiotics. The identification of a novel target to treat and to prevent shigellosis would alleviate the global burden of *Shigella* species.

Shigella species are members of the *Enterobacteriacae* family and classified into four species based on serological differences; *Shigella dysenteriae* (Group A), *Shigella flexneri* (Group B), *Shigella boydii* (Group C), and *Shigella sonnei* (Group D) (Lan & Reeves, 2002). *S. dysenteriae* type 1 encodes an exotoxin, shiga toxin, causing the most severe form of shigellosis, and it is responsible for most *Shigella*-related epidemics in Africa and Asia (Bhattacharya *et al*., 2003). *S. sonnei* is responsible for most shigellosis cases in developed countries. This is thought to be a result of improved drinking water conditions, where cross-reactive *Plesiomonas shigelloides* have been eliminated, causing a reduction in passive immunity against *S. sonnei* (Thapar & Sanderson, 2004). *S. flexneri* is responsible for most shigellosis in developing countries, is the most frequently isolated *Shigella* spp. and is the most frequent cause of shigellosis-related morbidity and mortality (Ram *et al*., 2008). Because of their disease severity, and frequency, *S.*

dysenteriae and *S. flexneri* are labeled as the biggest public health threat of all *Shigella* species (Kotloff *et al*., 1999). *S. flexneri* is most commonly used to study the mechanism of *Shigella* pathogenesis and is used in this study.

2. *Shigella flexneri* pathogenesis

Upon host ingestion of fecal contaminated food or water, *S. flexneri* travels through the digestive tract to the large intestine, where infection starts and the damage associated with shigellosis occurs (Schroeder & Hilbi, 2008). Once in the colon, *S. flexneri* is transcytosed through epithelial M-cells to the basolateral side of the epithelium where invasion begins (Sansonetti *et al*., 1996) (Figure 1). The bacteria can be endocytosed by macrophages; however, the bacteria induce rapid pyroptosis of the macrophages, allowing the bacteria access to the basolateral face of the colonic epithelium (Zychlinsky *et al*., 1992).

Shigella spp. are closely related to *Escherichia coli*, but encode a number of accessory virulence determinants, many of which are encoded on a large plasmid (Sansonetti *et al*., 1982), that give them the ability to have an intracellular life. The process by which *S. flexneri* infects human epithelial cells is highly controlled and complex. Regulation of infection is governed by a multi-step gene cascade containing three plasmid encoded virulence master regulators *virF, virB,* and *mxiE* (Makino *et al*., 1986; Sansonetti *et al*., 1982). *virF* is activated by increased temperature (37°C), low pH, and changes in osmolality; repression of *virF* by the nucleoid factors H-NS is alleviated upon intestinal tract entry (Schroeder & Hilbi, 2008; Tobe *et al*., 1991), resulting in expression of the major virulence master regulator VirF.

VirF induces expression of the actin polymerization gene *icsA* and of a second virulence master regulator, *virB*. VirB activates expression of genes that are required for host cell entry, including the Type Three Secretion System (T3SS) machinery and the primary effector proteins (Adler *et al*., 1989). Invasion of host epithelial cells begins when *S. flexneri* touches the basolateral side of the colonic epithelium and injects primary

effector proteins into host cell cytoplasm through the T3SS (High *et al*., 1992). Primary effector proteins induce host cytoskeletal rearrangement and bacteria are phagocytosed into a host vacuole. The vacuole is lysed, releasing the bacteria into the host cell cytoplasm. Dumping of effector proteins relieves repression of the third master virulence regulator *mxiE* (Sansonetti, 2001). MxiE activates the expression of secondary effector proteins encoded in the *mxiE* regulon, and upon translation, these proteins are immediately released through the T3SS (Mavris *et al*., 2002).

Once in the host cytoplasm, *S. flexneri* rapidly replicates, and moves via IcsA-mediated host actin polymerization (Bernardini *et al*., 1989; Goldberg & Theriot, 1995; Sansonetti, 2001). Re-activation of the T3SS is required to initiate infection of adjacent cells (Dragoi & Agaisse, 2015; Kuehl *et al*., 2014; Page *et al*., 1999) (Figure 1). The process of cell-to-cell spread repeats, and epithelial cells infected with *S. flexneri* eventually undergo necrosis. This results in a painful inflammatory immune response, and ulcer formation.

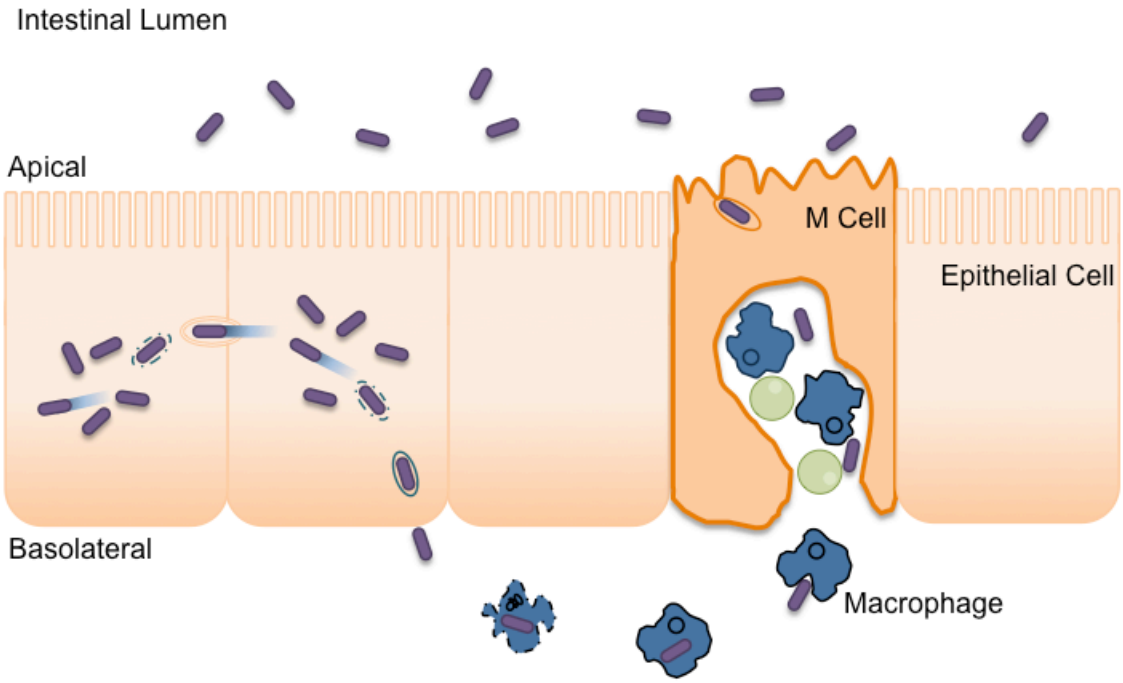

Figure 1. Schematic of *S. flexneri* pathogenesis.

Shigella is acquired through the ingestion of fecal contaminated substances. Once *Shigella* reaches the large intestine, it is transcytosed to the basolateral face of the intestinal epithelium, and invades using a specialized T3SS. *Shigella* spreads intercellularly by rapidly growing and moving using a specialized actin polymerization protein IcsA.

2.1 MECHANISMS USED TO STUDY *S. FLEXNERI* PATHOGENESIS.

In vitro cell culture models have been used extensively to study the stages of *S. flexneri* infection. Human epithelial cells lines, such as Henle-407, are infected with *S. flexneri* and stained with Giemsa to visualize cell invasion (Figure 2A) (Hale & Formal, 1981). Alternatively, spread can be measured using plaque assays where Henle-407 monolayers are infected and stained with Giemsa after an extended period of time (Figure 2B) (Oaks *et al*., 1985).

Genes encoded on the *S. flexneri* virulence plasmid have been extensively studied and are well characterized for their role in pathogenesis. The mechanism by which *S. flexneri* uses its T3SS to invade host tissue has been characterized, and, more recently, the dynamic process of intercellular spread is becoming better understood. Studies have shown that intercellular spread by *S. flexneri* is T3SS dependent (Allaoui *et al*., 1992; 1993; 1995; Andrews *et al*., 1991; Venkatesan *et al*., 1992), and mutants that are defective in actin polymerization are also unable to spread to adjacent host cells (Bernardini *et al*., 1989; Hong & Payne, 1997; Makino *et al*., 1986; Sandlin *et al*., 1995). However, many questions remain regarding the role of non-essential, chromosomal encoded genes in *S. flexneri* pathogenesis. Here, we take a closer look at these uncharacterized genes to understand their role in *S. flexneri* pathogenesis.

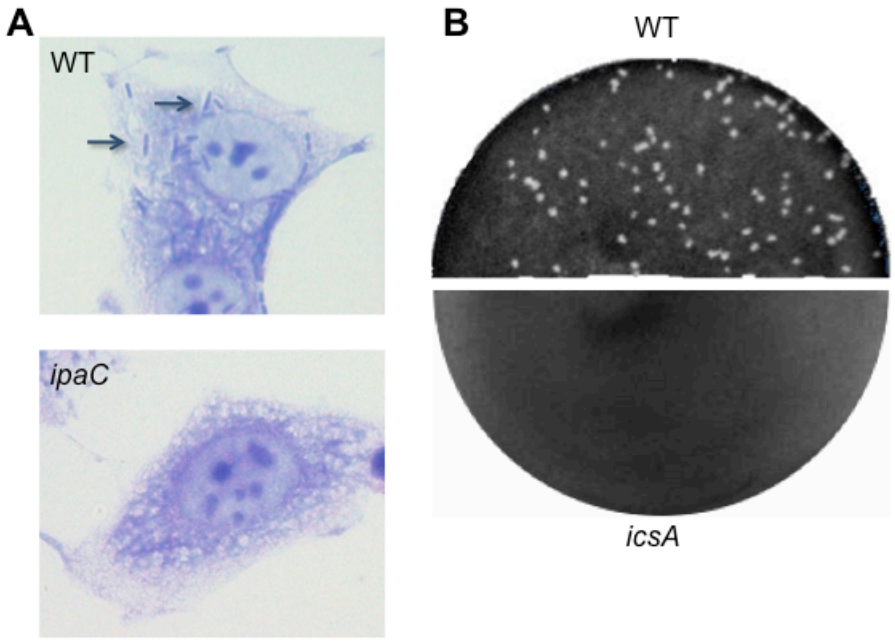

Figure 2. Cultured epithelial cells are used to study *S. flexneri* infection.

(A) *S. flexneri* T3SS is required for epithelial cell invasion. Semi-confluent monolayers of Henle-407 cells are infected with *S. flexneri* for 90 min and Giemsa stained to visualize bacteria within the cytoplasm. (B) *S. flexneri* IcsA is required for cell-to-cell spread. Confluent monolayers of Henle-407 cells are infected with *S. flexneri* for 72 hr, and Giemsa stained to visualize bacterial plaque formation indicating cell-to-cell spread (Oaks *et al*., 1985).

3. The Gram-negative bacterial membrane

In order for *S. flexneri* to successfully cause disease it must be able to quickly adapt to survive a wide variety of environments, such as the acidic environment of the stomach and intracellular environment of epithelial cells. Because *S. flexneri* is a Gram-negative bacteria (Schroeder & Hilbi, 2008), the outer membrane serves as the first line of defense against environmental stress (Needham & Trent, 2013). The Gram-negative bacterial cell envelope consists of a double membrane separated by a periplasmic space containing a thin peptidoglycan cell wall (Figure 3) (Silhavy *et al*., 2010). The outer membrane is asymmetrically composed of a lipopolysaccharide outer leaflet and a phospholipid inner leaflet, and the inner membrane is composed of a phospholipid bilayer (Schwechheimer & Kuehn, 2015).

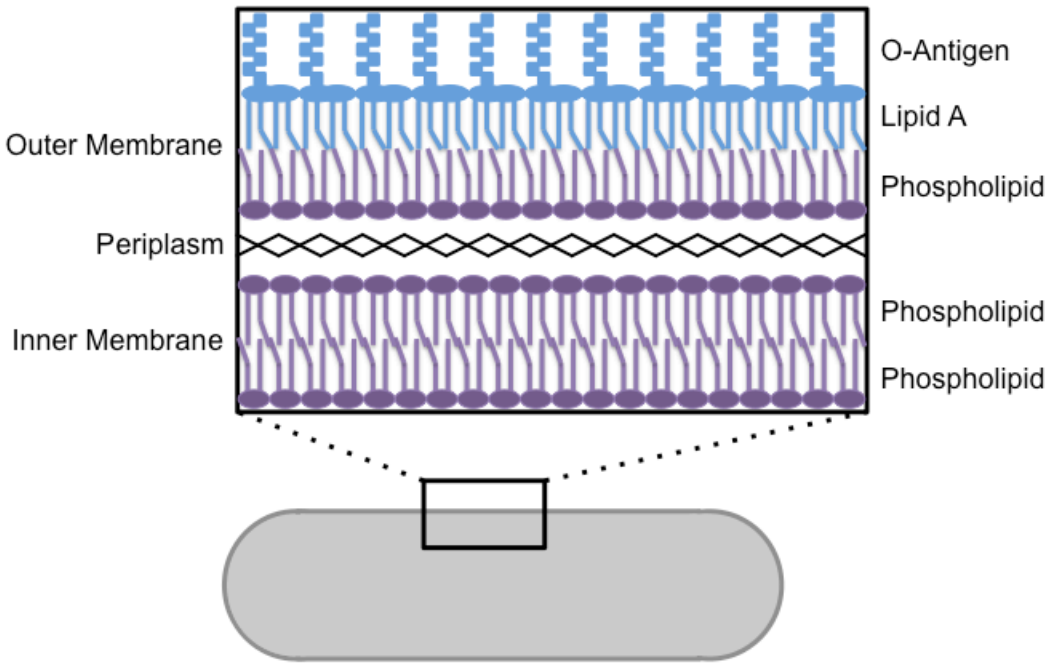

Figure 3. Schematic of the Gram-negative bacterial membrane.

The Gram-negative outer membrane is asymmetrically made up of outer leaflet lipopolysaccharide, containing an O-antigen chain anchored into the membrane by Lipid A, and inner leaflet phospholipids. Between the outer and inner membrane is the periplasmic region, containing a thin peptidoglycan layer. The bacterial inner membrane is made symmetrically of phospholipids. Figure adapted from Schwechheimer and Kuehn (2015).

3.1 LIPOPOLYSACCHARIDE.

The outer leaflet of the *S. flexneri* outer membrane is made up of lipopolysaccharide (Clifton *et al*., 2013). The bacterial lipopolysaccharide is composed of a lipid A molecule embedded in the bacterial outer membrane, connected to an O-antigen chain that masks the surface of the bacteria (Kamio & Nikaido, 1976). The lipopolysaccharide molecules of bacteria are most notable for their endotoxic affect and for their ability to activate a TLR4 response during infection (Raetz *et al*., 2007). Both the O-antigen chain and Lipid A molecules play important roles in *S. flexneri* pathogenesis.

The O-antigen chain of *S. flexneri* has been well characterized for its role in IcsA localization, while the role of the *S. flexneri* lipid A molecule in pathogenesis is less well understood. During pathogenesis, *S. flexneri* actively modifies the acylation state of its lipid A species during intracellular growth (Paciello *et al*., 2013). This phenotype has been observed in many Gram-negative bacteria and may help to evade the host immune response (Needham & Trent, 2013).

In other cases, modifications to the Gram-negative lipid A molecules can help to provide a barrier against harsh environmental conditions (Giles *et al*., 2011), or to gain resistance against antimicrobial peptides (Hankins *et al*., 2012). In *S. flexneri*, a mutation of *vpsC*, a component of the Mla pathway (Malinverni & Silhavy, 2009), causes an accumulation of phospholipids in the outer leaflet of the outer membrane (Carpenter & Payne, 2014). PagP activation causes remodeling of the *S. flexneri* lipid A species from hexa-acylated to hepta-acylated to reduce the amount of outer leaflet phospholipids; however, this modification to lipid A reduces the outer membrane integrity of *S. flexneri*, and this decreases intercellular spread of *S. flexneri*.

3.2 PHOSPHOLIPIDS.

Phospholipids make up the majority of *S. flexneri*'s membranes. The phospholipid bilayer makes up the bacterial inner membrane and the inner leaflet of the outer membrane. In general, relatively little is known of the role of specific phospholipids during bacterial pathogenesis, and their role in *S. flexneri* pathogenesis is unstudied.

Previous studies in the *S. flexneri*-like bacterium *E. coli* have determined the phospholipid composition of Gram-negative bacteria (Figure 4). During growth in exponential phase, phosphatidylethanolamine (PE) is the major phospholipid in the membrane of *E. coli,* representing almost 80% of the total phospholipids (Pluschke *et al*., 1978). The anionic phospholipids phosphatidylglycerol (PG) and cardiolipin account for about 18% and 2.5%, respectively (Pluschke *et al*., 1978).

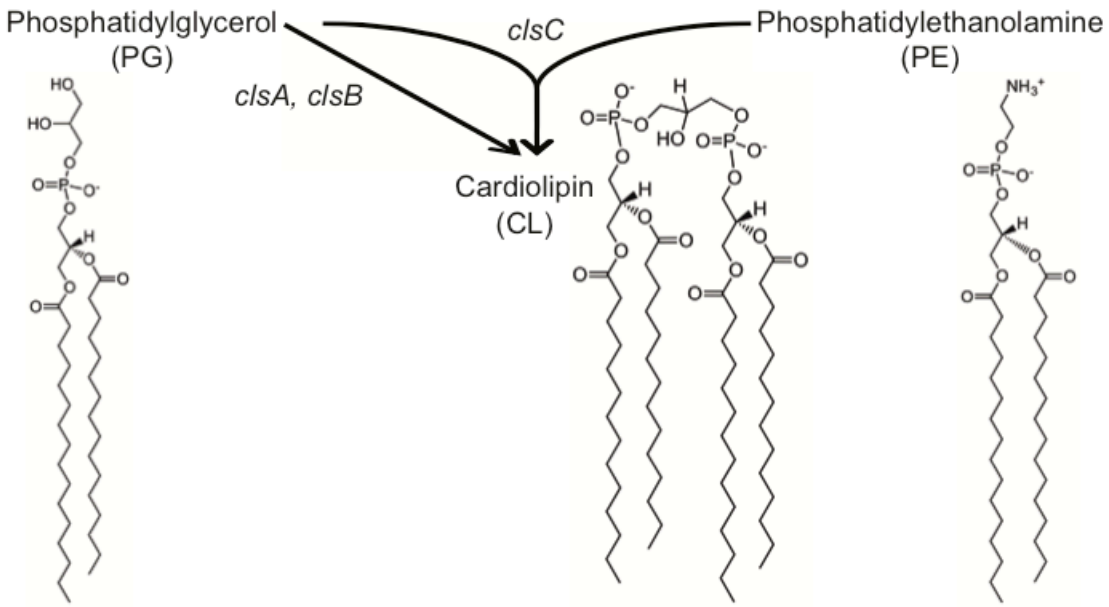

Figure 4. Schematic of *E. coli* cardiolipin synthesis.

In *E. coli*, cardiolipin (CL) is synthesized by the condensation of two phosphatidylglycerol (PG) molecules (*clsA* and c*lsB*) (Guo & Tropp, 2000; Pluschke *et al*., 1978) or the condensation of one PG and one phosphatidylethanolamine (PE) molecule (*clsC*) (Tan *et al*., 2012). The chemical structures of PG, PE, and CL were produced using ChemDraw (PerkinElmer). Figure taken from Rossi *et al*. (2017).

3.3 ANIONIC PHOSPOLIPIDS HAVE UNIQUE CHARACTERISTICS.

The anionic phospholipids of *E. coli* contain negatively charged glycerol head groups attached to phospho-glycerol molecules that connect two acyl chains. Anionic phospholipids tend to localize at the bacterial poles. Cardiolipin localizes to the bacterial pole (Figure 5), and phosphatidylglycerol localizes adjacent to cardiolipin (Oliver *et al*., 2014). In the absence of cardiolipin, the anionic phospholipid phosphatidylglycerol, which shares the same glycerol head group as cardiolipin, will localize to the bacterial poles (Renner & Weibel, 2011) and interact (Renner & Weibel, 2012) with proteins in a similar manner as cardiolipin.

Although anionic phospholipids only make up about 20% of the Gram-negative bacterial membrane, they are critical for maintaining the membrane structure. Anionic phospholipids are the point of attachment for the Braun lipoprotein, (Braun, 1975) a protein that connects the outer membrane to the inner membrane to prevent the outer membrane from sloughing away. Because of their unique localization and function, anionic phospholipids are thought to provide a mechanism for bacteria to localize proteins to organized membrane domains (Ramamurthi & Losick, 2009).

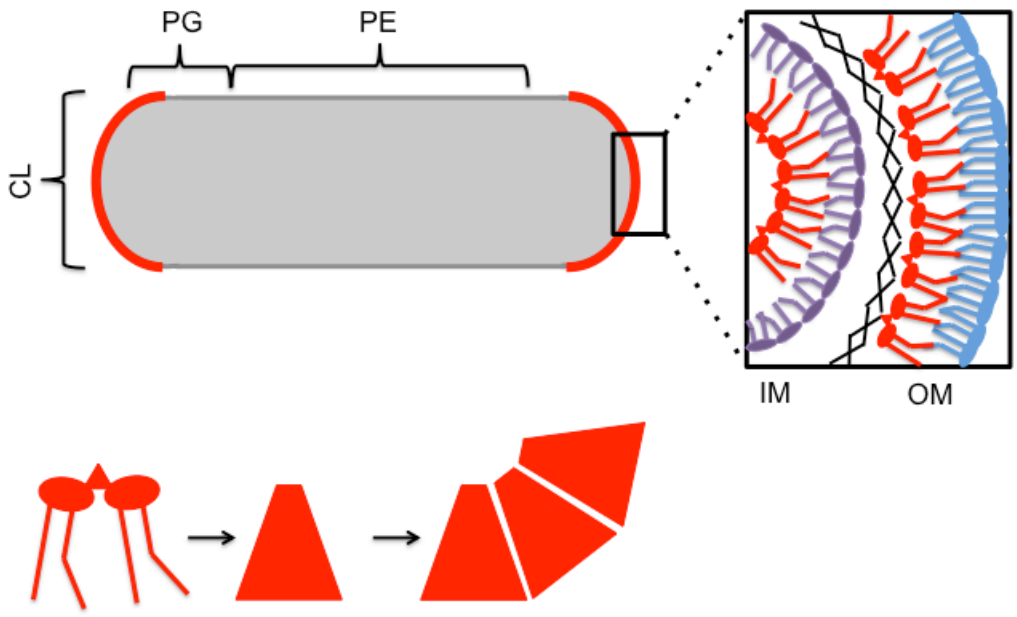

Figure 5. The misbalanced composition of cardiolipin allows it to localize at the bacterial poles.

Cardiolipin (CL) has a small glycerol head group connecting four large acyl chains. This gives cardiolipin a misbalanced composition and causes the destabilization of linear membranes. Cardiolipin, therefore, diffuses to the bacterial pole where regions of negative membrane curvature are found, in the inner leaflets of both the inner and outer membrane. In the region directly adjacent to the bacterial pole, phosphatidylglycerol (PG) is found, while phosphatidylethanolamine (PE) makes up the majority of the non-polar bacterial membrane. Adapted from Oliver *et al*. (2014).

4. Cardiolipin

In *E. coli*, cardiolipin appears to localize at the poles of the bacterial inner leaflets in both the inner and outer membranes (Oliver *et al*., 2014). Cardiolipin is a large anionic glycerol phospholipid composed of four large acyl chains connected by a small glycerol head group (Mileykovskaya *et al*., 2005). The composition gives cardiolipin a conical shape that allows it to accumulate at membrane regions that have negative curvature (Figure 5) (Renner & Weibel, 2011).

4.1 Identification of cardiolipin.

Cardiolipin was first identified in bovine cardiac tissue, which contains high proportions of mitochondria (Pangborn, 1945). Cardiolipin makes up the majority of the phospholipids found in the highly folded negative membrane curvature of the inner mitochondrial matrix and aids in the localization and activation of electron transport proteins (Mileykovskaya *et al*., 2005). Further analysis determined that cardiolipin helps to orient proteins for proper protein-protein interactions to shuttle electrons (Schenkel & Bakovic, 2014).

4.2 Role in bacterial membrane.

The functional characteristics of cardiolipin observed in the inner mitochondrial membrane have also been observed in the plasma membrane of *E. coli*. Here, cardiolipin can also localize electron transport proteins for their activation (Yankovskaya *et al*., 2003). In addition, cardiolipin has also been implicated in the osmotic stress response of both Gram-negative and Gram-positive bacteria (Koprivnjak *et al*., 2011; Lin *et al*., 2015; López *et al*., 2006; Romantsov *et al*., 2009; Subramani *et al*., 2016), suggesting

cardiolipin aids in localizing osmotic transport proteins within the plasma membrane (Romantsov *et al*., 2009). Cardiolipin has also been shown to be important for the localization and activation of proteins required for cell division (Hsieh *et al*., 2010).

4.3 ROLE IN BACTERIAL PATHOGENESIS.

Until recently, the role of cardiolipin in bacterial pathogenesis has been under studied. This is likely because most bacteria have three-cardiolipin synthases, so all three must be deleted to see a cardiolipin-associated phenotype. In addition, the absence of cardiolipin may be functionally compensated for by the other anionic phospholipid, phosphatidylglycerol. As a result, most bacteria that lack cardiolipin do not display an in vitro growth phenotype.

In *Moraxella catarrhalis*, cardiolipin has been shown to be required for proper adherence to human epithelial cells (Buskirk & Lafontaine, 2014), suggesting that cardiolipin aids in the localization of adhesion proteins that are required for pathogenesis. In *Salmonella enterica* Typhimurium, PbgA transport cardiolipin to the outer membrane (Figure 6), and this is required for intracellular survival within macrophages (Dalebroux *et al*., 2015), suggesting that cardiolipin is required to maintain barrier integrity in the harsh environment of the phagosome.

The role of cardiolipin in *S. flexneri* pathogenesis is unknown.

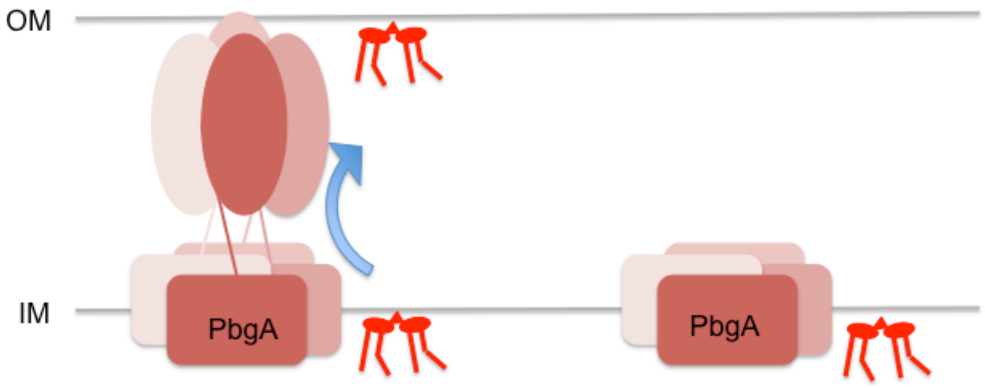

Figure 6. Schematic of *S*. Typhimurium transport of cardiolipin to the outer membrane.

In *S*. Typhimurium, cardiolipin is transported to the bacterial outer membrane by PbgA (Dalebroux *et al*., 2015). In response to PhoPQ inducing conditions, expression of *pbgA* increases and PbgA oligomerizes within the bacterial inner membrane. This allows delivery of cardiolipin to the outer membrane, via the PbgA periplasmic domain. Removal of this C-terminal periplasmic domain inhibits cardiolipin transport. Figure adapted from Dalebroux *et al*. (2015).

5. Overview of *S. flexneri* IcsA

S. flexneri, which is non-motile, uses actin-based propulsion to move through the host cell cytoplasm and protrude into the neighboring cell. Actin-based motility requires proper localization of the virulence protein IcsA to one pole on the bacterial surface (Goldberg *et al*., 1993; 1994). During invasion, IcsA contributes to bacterial uptake by aiding in the adhesion of the bacteria to the host epithelial cell (Brotcke Zumsteg *et al*., 2014). Once inside the host cell cytoplasm, IcsA is responsible for the recruitment of neural Wiskott-Aldrich syndrome protein (N-WASP) found in the host cell cytosol (Egile *et al*., 1999; Suzuki *et al*., 2002). N-WASP then recruits Arp2/3, activating actin-based motility. IcsA mutants are invasive and replicate within epithelial cells but cannot spread to adjacent cells (Bernardini *et al*., 1989).

IcsA is a member of the auto-transport protein family (Figure 7A) (Kühnel & Diezmann, 2011). It contains an N-terminal signal sequence that allows for secretion from the cytoplasm to the periplasm (Suzuki *et al*., 1995). Adjacent to the secretion signal is a passenger domain. This domain contains functional domains of IcsA including the following: the N-WASP recruitment domain (Teh & Morona, 2013), polar targeting (PT) domain (Charles *et al*., 2001), passenger-associated transport repeats (Doyle *et al*., 2015c), and IcsP cleavage site (Fukuda *et al*., 1995). The C-terminal domain contains the beta-barrel (Leyton *et al*., 2012), which integrates into the bacterial outer membrane for passenger domain surface exposure.

Translation of IcsA occurs in the cytoplasm, and its N-terminal signal sequence directs IcsA secretion into the periplasm through the inner membrane Sec system (Figure 7B) (Brandon *et al*., 2003). During secretion, this N-terminal signal sequence of IcsA is

cleaved. Once in the periplasm, IcsA transitions to the outer membrane where the C-terminal beta-barrel then inserts into the outer membrane. Rapid auto-transport of the IcsA passenger domain then occurs, exposing the passenger domain to the outside of the bacterial cell.

The localization of IcsA on the surface of *S. flexneri* is to the old pole of the bacterial cell (Goldberg *et al*., 1993); however, the mechanism for unipolar targeting of IcsA is complex and incompletely understood (Agaisse, 2016).

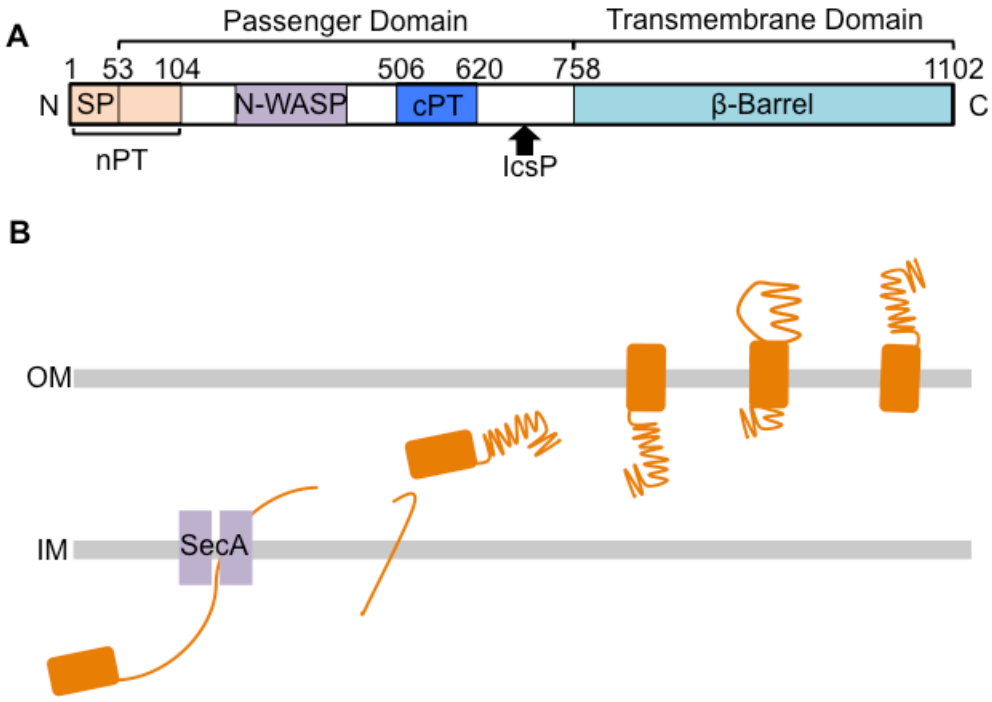

Figure 7. Schematic of *S. flexneri* IcsA.

(A) IcsA contains two major domains. At the N-terminus is the passenger domain, containing the secretion signal sequence, N-WASP recruitment domain, and domain required for polar targeting of IcsA. The C-terminus contains the beta-barrel domain, which is inserted into the bacterial outer membrane and allows for auto-transport and extracellular exposure of the passenger domain. Figure adapted from Doyle *et al.* (2015a). (B) IcsA is transcribed in the cytoplasm and secreted into the periplasm via the inner membrane Sec system. Once in the periplasm, the IcsA beta-barrel inserts into the outer membrane, followed by rapid auto-transport of the passenger domain for extracellular exposure. Figure adapted from Brandon and Goldberg (2011).

6. Mechanisms for IcsA localization

6.1 Role of chaperone proteins in IcsA localization.

During its translation in the cytoplasm and secretion to the periplasm, the IcsA beta-barrel remains in a folded conformation (Brandon & Goldberg, 2001); however, the passenger domain remains unfolded in the cytoplasm and becomes properly folded in the periplasm. Cytoplasmic chaperone proteins, such as DnaK (Janakiraman *et al*., 2009) and YidC (Gray *et al*., 2014), help IcsA remain in the proper conformation in the cytoplasm to facilitate periplasmic secretion. DnaK itself localizes to the bacterial pole and facilitates secretion of IcsA to the periplasm at the bacterial pole (Janakiraman *et al*., 2009).

Once in the periplasm, the beta-barrel of IcsA must remain folded, and the passenger domain of IcsA must become properly folded (Brandon & Goldberg, 2001). Periplasmic chaperone proteins DegP, Skp, and SurA have been shown to be required for unipolar surface localization of IcsA (Purdy *et al*., 2002; 2007). This suggests that these chaperone proteins aid in the periplasmic folding of IcsA or targeting of IcsA to the bacterial pole for outer membrane insertion and auto-transport.

6.2 Role of O-antigen in IcsA localization.

Lipopolysaccharide is the major component of the *S. flexneri* outer membrane (Kenne *et al*., 1978). The O-antigen polysaccharide chain that is connected to the lipid A region of the *S. flexneri* lipopolysaccharide is responsible for providing a smooth bacterial surface (Simmons & Romanowska, 1987). The O-antigen chain length of *S. flexneri* is bi-modal, and the modal composition is species dependent (Brahmbhatt *et al*.,

1992). Early studies showed that *S. flexneri* rough mutations that lack the O-antigen chain of the lipopolysaccharide are associated with disruption of IcsA localization (Hong & Payne, 1997; Morona *et al*., 1995); however, the mechanism is unknown.

One model suggests that the presence of O-antigen can affect the membrane fluidity of the bacterial outer membrane. In the presence of O-antigen, the membrane fluidity is low, resulting in less IcsA diffusion from the bacterial pole (Robbins *et al*., 2001). In the absence of O-antigen, the membrane fluidity is high, increasing IcsA diffusion from the bacterial pole. An alternative model for O-antigen directing IcsA polar localization suggest localization of IcsA is dependent on the spatial localization of short and long O-antigen. An increase in O-antigen length, observed at the non-polar regions of the bacteria, could shield IcsA to inhibit its function (Morona & Van Den Bosch, 2003), whereas a decrease in O-antigen chain length, observed at the bacterial pole, could unmask IcsA for proper function (Sandlin *et al*., 1995).

A more recent study showed that IcsA polarity and surface diffusion is not affected by O-antigen composition (Doyle *et al*., 2015a). In addition, they showed that O-antigen chain length are symmetrical across the bacterial surface, therefore IcsA masking is symmetrical. This has lead to a more recent model suggesting that O-antigen synthesis can regulate IcsA levels, thereby effecting IcsA polarity (Doyle *et al*., 2015a).

6.3 ROLE OF OUTER MEMBRANE PROTEINS IN ICSA LOCALIZATION.

6.3.1 IcsP.

The major *S. flexneri* outer membrane protease, IcsP, is required for cleavage of surface exposed IcsA. (Shere *et al*., 1997). Located near the C-terminal portion of the IcsA passenger domain is an IcsP cleavage site (Shere *et al*., 1997). This cleavage mediates the turnover of IcsA from an active to inactive form by releasing the 95-kD N-terminal domain of IcsA. Interestingly, the localization of IcsP is opposite to that of *S. flexneri* IcsA (Tran *et al*., 2013), where IcsP localizes to the bacterial septum which becomes the new pole. This suggests that IcsP controls unipolar exposure of the IcsA N-WASP recruitment domain by cleaving IcsA that is exposed at the new pole of *S. flexneri*.

Polar localization of IcsA when expressed in bacteria that lack characterized *S. flexneri* systems thought to be involved in IcsA localization, such as IcsP (Robbins *et al*., 2001; Tran *et al*., 2013), still have a large proportion of polar localized IcsA, suggesting intrinsic protein properties of IcsA cause polar localization.

6.3.2 OmpA and PhoN2.

The major outer membrane protein of *S. flexneri*, OmpA, which is circumferentially localized, has been shown to play a role in IcsA localization (Ambrosi *et al*., 2012). In the absence of OmpA, IcsA is exposed uniformly across the bacterial surface; however, actin tails are still produced. Further studies revealed that the *S. flexneri* OmpA is found in two conformations, and it was hypothesized that polar OmpA is in a different conformation than the non-polar OmpA.

Recently, the periplasmic apyrase protein, PhoN2 (Santapaola *et al*., 2006), has been shown to localize to the bacterial pole and interact with OmpA but not IcsA (Scribano *et al*., 2014; 2016). In addition, targeting of PhoN2 was independent of OmpA, and polar conformation of OmpA disappeared in the absence of PhoN2. This suggests that the interaction between of PhoN2 on OmpA keeps OmpA in its polar conformation and results in IcsA exposure. However, the mechanism PhoN2 uses to localize to the bacterial pole is unknown.

6.4 ROLE OF ICSA POLAR TARGETING DOMAIN IN ICSA LOCALIZATION.

Intrinsic polar targeting domains have been identified within IcsA (Figure 8A). For example, the N-terminal (IcsA 1-104) and central (IcsA 507-620) polar targeting regions (Charles *et al*., 2001), when fused to fluorescent proteins, are able to direct fluorescence to the poles of *S. flexneri* and other Gram-negative bacteria (Doyle *et al*., 2015b; Janakiraman *et al*., 2009). Because these IcsA fusion proteins do not contain the N-terminal secretion domain of IcsA, it suggests these domains can target IcsA to the pole independent of periplasmic secretion, suggesting a conserved method for polar targeting between the inner and outer membrane.

Mutational analysis of the central polar targeting domain for residues that disrupt polar targeting reveled two residue "hot-spot" areas (HS1 - IcsA 522-535 and HS2 – IcsA562-567) (Doyle *et al*., 2015b; May & Morona, 2008). Further analysis of these mutants revealed that polar targeting, in most mutants, was affected because of reduced IcsA levels. This suggest that these mutations are affecting the stability of IcsA, not polar targeting. However, a mutation in IcsA-Arg546 (Figure 8B) resulted in reduced polar

targeting of IcsA, and this effect was independent of IcsA protein levels suggesting Arg564 plays a role in bringing IcsA to the bacterial pole.

Recently, the crystal structure of the IcsA passenger domain was resolved (Leupold *et al*., 2017), providing insight into the role of each polar targeting domain mutation on the IcsA structure. The structural characteristics of the IcsA passenger domain containing the central polar targeting domain are consistent with a beta-helix. Residues in the HS2 domain, required for IcsA polar targeting, are required to maintain the hydrophobic core of the beta-helix. Mutations in these residues are predicted to lead to protein instability and reduced levels of IcsA. Interestingly, IcsA-Arg564 was found to be an exposed residue in the HS2 domain, and a mutation in this residue is not predicted to alter the stability of the hydrophobic core. Together, these data suggest that IcsA-Arg564 is the critical residue directing the central polar targeting domain of IcsA.

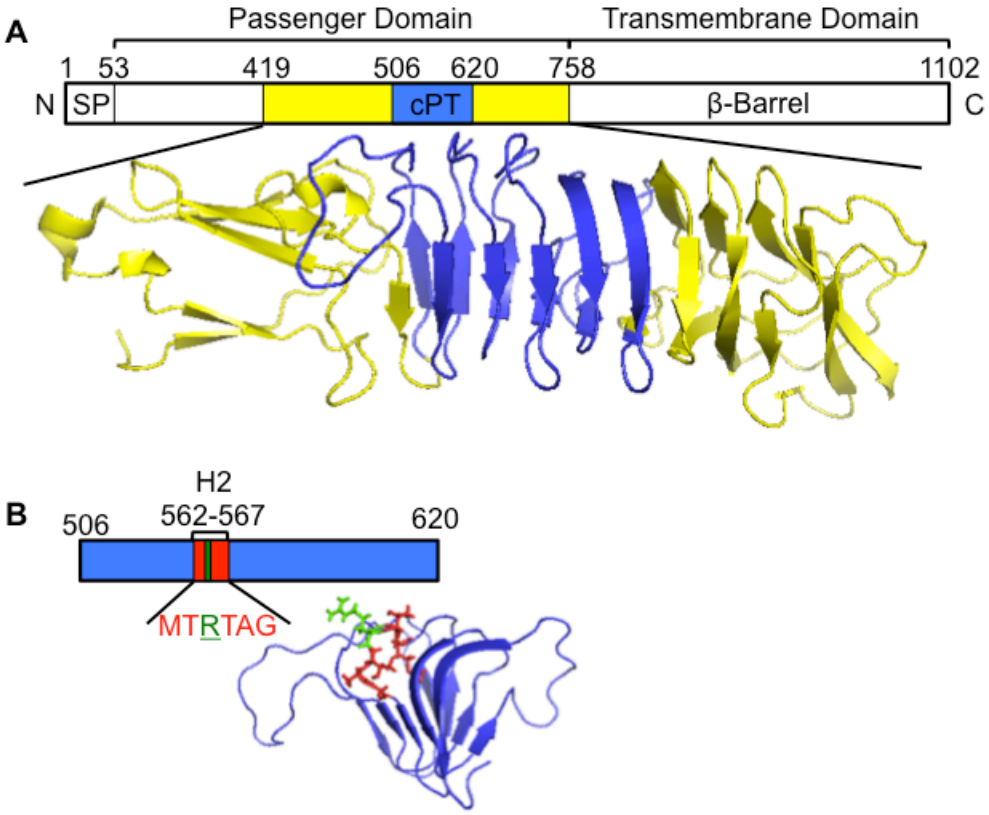

Figure 8. IcsA-Arg564 is critical for IcsA polar targeting.

(A) IcsA is an auto-transport protein. It contains an N-terminal signal peptide (SP), a passenger domain that consists of a polar targeting region (PT), and a C-terminal beta-barrel transmembrane domain. Figure adapted from Leupold *et al*. (2017). (B) Residues in Hot Spot 2 (H2) are required for polar targeting of IcsA. IcsA-Arg564 in H2 is exposed and critical for polar targeting, independent of IcsA structure. Figure adapted from Doyle *et al*. (2015a) and Leupold *et al*. (2017).

7. Purpose of this research

Worldwide, *Shigella spp*. infect hundreds of millions of people annually, with fatality rates up to 15%. Increasing antibiotic resistance between *Shigella* isolates compromises treatment of shigellosis, and there is no approved vaccine to prevent future infection. This has created a growing need to understand the molecular mechanism *Shigella* uses to cause disease and to identify therapeutic targets to treat and prevent future *Shigella* infections.

To cause disease, *S. flexneri* must encode the tools necessary to invade colonic epithelial cells, then replicate and move within host cell cytoplasm, and then spread intercellularly. Genes encoded on a large virulence plasmid have been well characterized for their role in *S. flexneri* pathogenesis; however, many chromosomally encoded genes, that are not required for in vitro growth, remain uncharacterized. This study examines the role of *S. flexneri* phospholipid composition in pathogenesis.

In this study I have established that cardiolipin is required for *S. flexneri* pathogenesis, although cardiolipin only makes up 7% of *S. flexneri* phospholipids. I determined that *clsA* encodes the major cardiolipin synthase, and *pbgA* encodes the phospholipid transporter in *S. flexneri*. Both of these genes were required for *S. flexneri* plaque formation but acted at different points in the virulence pathway. I determined that *S. flexneri* requires cardiolipin in the inner membrane for proper intracellular division, and outer membrane cardiolipin is required for unipolar localization of the actin polymerization protein IcsA.

This study contributes to our understanding of the intracellular lifestyle of *S. flexneri* and the mechanism it uses to localize virulence proteins. In addition, it

contributes to our understanding of the role of phospholipids, specifically cardiolipin, during bacterial pathogenesis. The lack of an in vitro phenotype displayed by cardiolipin deficient bacteria has caused it to be overlooked. This study should encourage re-examination of cardiolipin in other bacteria, as its synthesis and outer membrane transport pathways could be novel antimicrobial targets.

II. MATERIALS AND METHODS

1. Bacterial Media and Growth Conditions

All strains were maintained at -80°C in Tryptic Soy Broth (TSB) containing 20% (v/v) glycerol. *E. coli* strains were grown on Luria-Bertani (LB) agar (1% tryptone, 0.5% yeast extract, 1% NaCl, 1.5% agar [w/v]) at 37°C, and single colonies were selected and grown in LB broth at 37°C. *S. flexneri* strains were grown on TSB agar (TSB, 1.5% agar [w/v]) containing Congo red dye (0.01% [w/v]; Sigma) at 37°C. Congo red binding colonies (Payne & Finkelstein, 1977), indicating a functional T3SS, were selected and grown in LB broth at 30°C for maintenance, and were then subcultured 1:100 and grown at 37°C for assays. Antibiotics were used at the following concentrations: kanamycin, 50 μg/ml; ampicillin, 25 μg/ml.

2. DNA Techniques

2.1 DNA Isolation.

2.1.1 Chromosomal.

Bacterial chromosomes were isolated from 1.0 ml of overnight culture using the Invitrogen PureLink Genomic DNA kit. Chromosomes were stored in double distilled water (ddH_2O) at -20°C.

2.1.2 Plasmid.

Bacterial plasmids were isolated from 5.0 mls of overnight culture using the Sigma- Aldrich GenElute Plasmid Miniprep kit. Plasmids were stored in ddH_2O at -20 °C.

2.2 Polymerase chain reaction.

Primers used in this study are listed in Table 1.

2.2.1 Amplification.

DNA amplifications were carried out using either Novagen KOD Hot Start DNA Polymerase High-Fidelity or New England Biolabs Phusion High-Fidelity DNA Polymerase. Templates used were either purified chromosomal DNA or plasmid DNA, at 50 ng and 10 ng per reaction, respectively.

For KOD, standard reaction conditions were used with an initial denaturing step at 95 °C for 2 min. This was followed by 30 cycles of: denaturing at 95 °C for 20 sec, annealing at varying temperatures depending on primers between 55 °C and 65 °C for 10 sec, and extension at 70 °C with varying extension times at 30 sec per kb depending on product length. Reaction was finished with a final 5 min extension at 70 °C and held at 4 °C until further use.

For Phusion standard reaction conditions were used with an initial denaturing step at 98 °C for 30 sec. This was followed by 30 cycles of: denaturing at 98 °C for 10 sec, annealing at varying temperatures depending on primers between 55 °C and 65 °C for 30 sec, and extension at 72 °C with varying extension times at 30 sec per kb depending on product length. Reaction was finished with a final 5 min extension at 72 °C and held at 4 °C until further use.

2.2.2 Screening.

To confirm proper chromosomal manipulation or plasmid construction, colony PCR was performed using New England Biolabs *Taq* DNA Polymerase. Standard reaction were used with an initial denaturing step at 98 °C for 30 sec. This was followed by 30 cycles of: denaturing at 95 °C for 30 sec, annealing at varying temperatures depending on primers between 55 °C and 65 °C for 30 sec, and extension at 68 °C with varying extension times of 1 min per kb depending on product length. Reaction was finished with a final 5 min extension at 68 °C and held at 4 °C until further use. Bacterial colonies were frozen in 50 µl of ddH_2O, and 1 µl of this suspension was used as PCR template.

2.2.3 Site-directed Mutagenesis.

Amino acid substitutions in expression plasmids were made using the Agilent Technologies, Inc. QuikChange protocol. Overlapping primers were designed to introduce a single codon substitution during PCR amplification. PCR reactions were carried out using the New England Biolabs Phusion High-Fidelity DNA Polymerase protocol. Standard reaction used (see above). After amplification, the product was treated with DpnI and transformed into chemically competent *E. coli* Top10 cells for screening.

Table 1. Primers used in this study.

Primer	Sequence (5' to 3')
clsA-F	GCTGACAGTAAAGAATCGGC
clsA-R	ATCGTAGGCCTGCTCAAGCG
pbgA-KO-F	CCGCATTCTTATTTATCGCCTTTATCGCCTCGCATGTGG TGTATATCTGAGTGTAGGCTGGAGCTGCTTC
pbgA-KO-R	TTCCACACCGATTGCAAGTAAGATATTTCGCTAACTGA TTTATAATTAATCATATGAATATCCTCCTTAG
pbgA-F	TAACGAGAATGATTTAACGC
pbgA-R	ATACTACCGTTTTCCACACC
IcsA-419-F	TGTTTAACTTTAAGAAGGAGATATACCATGGGCCATCA TCACCATCACCACGATTATGACATTCCGACGACGGAGA ACTTGTACTTCCAAGGAATTTGGCAACAATGTAAAAGT GGAGGC
IcsA-758-R	TGTTAGCAGCCGGATCCTCAGCGACTACTCATTTGAGT AGACTCTTGATTGC
IcsA-Arg564Ala-F	GGGGACAGTTGAAGCTATGACAGCTACCGCTGGTGTTA TTG
IcsA-Arg564Ala-R	CAATAACACCAGCGGTAGCTGTCATAGCTTCAACTGTC

Table 1 (continued).

	CCC
IcsA-502-F	AUGGTTAGTACTATTCTGGCAGATAATCTCAGCC
IcsA-620-R	TGCTGCTGCTGCTGCTGCTGCTGCACCGTTTTTCTCCAG AGTCATGTTACC
GFP-F	GGAGGAGGAGGAGGAGGAGGAGGAGGAGCTAGCAAA GGAGAAGAACTC
GFP-R	CTCAGTTGTACAGTTCATCCATGCC

2.3 PLASMID CONSTRUCTION.

Plasmids used in this study are listed in Table 2. Constructed plasmids were sequenced at the University of Texas at Austin DNA sequencing facility using an ABI 3130 sequencer (Applied Biosystems). Sequences were analyzed using SnapGene software.

2.3.1 p*clsA*.

A plasmid expressing *clsA* was constructed by amplifying the wild-type locus containing the native promoter region from *S. flexneri* strain 2457T and ligating the PCR product into the SmaI site of pWKS30 (Wang & Kushner, 1991). Primers clsA-F and clsA-R were used to amplify *clsA,* using *S. flexneri* genomic DNA as template (Wei *et al*., 2003).

2.3.2 p*pbgA*.

A plasmid expressing *pbgA* was constructed by amplifying the wild-type locus containing the native promoter region from *S. flexneri* strain 2457T and ligating the PCR product into the SmaI site of pWKS30 (Wang & Kushner, 1991). Primers pbgA-F and pbgA-R were used to amplify *pbgA*, using *S. flexneri* genome DNA as template (Wei *et al*., 2003).

2.3.3 p*icsA-gfp*.

A plasmid expressing *icsA*-502-620 with C-terminal *gfp* was constructed by amplifying the wild-type *icsA* locus from *S. flexneri* strain 2457T using primers IcsA-

502-F and IcsA-620-R, and then amplifying the *gfp* locus from pVES143 using primers GFP-F and GFP-R. Overlap PCR was then performed to produce a single fragment using individual *icsA* and *gfp* fragments as template and primers IcsA-502-F and GFP-R. The final PCR product was ligated into the SmaI site of pWKS30 (Wang & Kushner, 1991).

2.3.4 p*icsA*-His.

A plasmid expressing *icsA*-417-758 with a N-terminal 6xHis tag was constructed by amplifying the wild-type locus from *S. flexneri* strain 2457T using primers IcsA-419-F and IcsA758-R. The PCR product was ligated into the NcoI and BamHI sites of pET16b (Novagen).

2.3.5 p*icsA*-His-Arg564Ala.

A plasmid expressing *icsA*-419-758 with a N-terminal 6xHis tag and with Arg564 of *icsA* substituted to an Ala, was constructed by performing a quick change reaction on plasmid p*icsA*-His using primers IcsA-Arg564Ala-F and IcsA-Arg564Ala-R.

Table 2. Plasmids used in this study.

Plasmids	Description	Reference
pKD4	*kan* cassette template	(Datsenko & Wanner, 2000)
pKD46	Ts Red recombinase	(Datsenko & Wanner, 2000)
pCP20	Ts Flp recombinase	(Cherepanov & Wackernagel, 1995)
pWKS30	Low-copy expression vector	(Wang & Kushner, 1991)
pET16b	N-term His with TEV protein purification vector	Novagen
pVES143	GFP template vector	(Waters *et al*., 2008)
p*clsA*	*clsA* in pWKS30	This study
p*pbgA*	*pbgA* in pWKS30	This study
p*cfp*	*cfp*-expressing plasmid	(Dragoi & Agaisse, 2014)
p*yfp*	*yfp*-expressing plasmid	(Dragoi & Agaisse, 2014)
p*icsA*-His	*icsA* amino acids 419 -758 in pET16b with N-terminal His tag and TEV site	This study (Leupold *et al*., 2017)
p*icsA*-His-Arg564Ala	*icsA* amino acids 419 -758 in pET16b with N-terminal His tag and TEV site	This study

Table 2 (continued).

	with Arg 546 substituted to Ala	
p*icsA-gfp*	*icsA* amino acids 502-620 with C-terminal GFP fusion in pWKS30	This study (Doyle *et al*., 2015b)

3. Construction of Bacterial Strains

Strains used in this study are listed in Table 3. All mutations were verified via colony PCR.

3.1 TRANSFORMATION OF *E. COLI.*

$CaCl_2$-competent Top 10 *E. coli* cells were used for plasmid construction and maintenance by heat-shock transformation. Competent *E. coli* cells were prepared from mid-log (OD_{650}~ 0.4) cultures. The cultures were chilled and then pelleted at 4°C. The cells were washed with ice-cold $CaCl_2$solution (60 mM $CaCl_2$, 10 mM PIPES at pH 7.0, and 15% glycerol) and then incubated overnight in fresh $CaCl_2$ solution at 4°C. The cells were then pelleted at 4°C and resuspended in fresh $CaCl_2$ solution (concentrated 100X from culture volume) and divvied into 100 µl aliquots and stored at -80°C.

Transformations were carried out by thawing cells on ice, followed by an additional ice incubation with plasmid DNA for 20 min. Cells were then heat shocked at 42°C for 45 seconds, chilled on ice for 2 min and incubated with 750 µl of LB for 1 hour at 37°C. Bacteria were then plated on LB agar supplemented with antibiotics.

3.2 P1 TRANSDUCTION.

S. flexneri chromosomal mutations were generated by bacteriophage P1 transduction from *E. coli*. P1 bacteriophage stocks were maintained and titered on *E. coli* strain W3110 in LB soft agar (LB containing 0.75% agar and 5 mM $CaCl_2$), containing 1 mM dithiotreitol (DTT). *E. coli* donor strains (Baba *et al*., 2006) were grown in LB containing 5 mM $CaCl_2$ to late-log (OD_{650}~ 0.8). 100µl of culture and 100µl of $1x10^8$

pfu/ml P1 stock was added to soft agar, overlaid onto LB agar and incubated at 37°C. Upon lysis of the bacterial lawn, the P1 was harvested by adding 2ml LB, containing 5 mM $CaCl_2$, to the soft agar, for collection, and a few drops of chloroform. The soft agar/chloroform mixture was vortexed for 1 min, and cell debris was pelleted. P1 donor supernatant were collected and stored at 4°C with chloroform. P1 donor was titered prior to recipient transduction.

Recipient *S. flexneri* strains were grown in LB containing 5 mM $CaCl_2$ to mid-log (OD_{650} ~ 0.4) and 100µl of $1x10^8$ pfu/ml P1 donor was added to 1 ml of recipient culture and incubated at 37°C for 1 hour. Cells were then pelleted, resuspended in LB containing 50 mM Na-citrate, and incubated at 37°C for 1 hour. *S. flexneri* recipients were then plated on TSB agar containing antibiotics.

3.3 ELECTROPORATION.

Electroporation was used to transform plasmid DNA into *S. flexneri*. Electrocompetent *Shigella* were prepared from mid-log (OD_{650} ~ 0.4) cultures. The cultures were pelleted and washed twice with ice cold G-buffer (137 mM sucrose, 1 mM HEPES, pH 8). The cultures were then resuspended into 500µl of G-buffer and transferred into cold electroporation cuvettes (BioRad). Plasmid DNA was added and *S. flexneri* was electroporated using a GenePulse electroporator (BioRad) with the following settings; 200 Ω, 25 mF, and 2.5 V. Bacteria were then incubated in 750µl of LB for 1 hour at 37°C, and grown on TSB agar with antibiotics.

3.4 CONSTRUCTION OF *S. FLEXNERI* STRAINS.

3.4.1 *clsA*.

The *S. flexneri clsA* mutant was created by bacteriophage P1 transduction of the *ΔclsA:kan* allele from *E. coli* strain JW1241 (Keio Collection) into *S. flexneri* 2457T 2a (Baba *et al*., 2006).

3.4.2 *clsB*.

The *S. flexneri clsB* mutant was created by bacteriophage P1 transduction of the *ΔclsB:kan* allele from *E. coli* strain JW0772 (Keio Collection) into *S. flexneri* 2457T 2a (Baba *et al*., 2006).

3.4.3 *clsC*.

The *S. flexneri clsC* mutant was created by bacteriophage P1 transduction of the *ΔclsC:kan* allele from *E. coli* strain JW5150 (Keio Collection) into *S. flexneri* 2457T 2a (Baba *et al*., 2006).

3.4.4 *clsA*, *clsB*, and *clsC* double and triple mutants.

Double and triple mutants were created using a multi-step procedure where by the kanamycin resistance cassette used to create an existing mutation was removed using the plasmid pCP20 (Cherepanov & Wackernagel, 1995), followed by P1 transduction to mutate additional genes.

3.4.5 *pbgA*.

The *S. flexneri pbgA* mutant was created using λ-Red-mediated recombination (Datsenko & Wanner, 2000). A PCR product was generated by amplifying the kanamycin resistance cassette from pKD4 using primers pbgA-KO-F and pbgA-KO-R, which modified the wild-type *pbgA* gene by introducing a UGA termination codon in place of the codon for Y190 and replaced the downstream codons with a kanamycin resistance cassette (Datsenko & Wanner, 2000; De Lay & Cronan, 2008). This PCR product was introduced by electroporation into *E. coli* strain BW25113 expressing λ-Red-recombinase from plasmid pKD46 (Datsenko & Wanner, 2000), and recombinants were selected by kanamycin resistance. This mutation was then introduced into *S. flexneri* through bacteriophage P1 transduction.

Table 3. Strains used in this study.

Strain	Description	Reference
E. coli		
Top10	Cloning strain	Thermo Fisher Scientific
W3110	Wild Type	(Oliver *et al*., 2014)
BL 21 DE3	Protein purification strain	New England Biosciences
BW25113	Wild Type	(Datsenko & Wanner, 2000)
JW1241	BW25113 *Δcls*::*kan*	Keio Collection (Baba *et al*., 2006)
JW0772	BW25113 *ΔybhO*::*kan*	Keio Collection (Baba *et al*., 2006)
JW5150	BW25113 *ΔymdC*::*kan*	Keio Collection (Baba *et al*., 2006)
JW3160	BW25113 *ΔmlaD*::*kan*	Keio Collection (Baba *et al*., 2006)
E.C.-pbgA	BW25113 *ΔyejM190-586*::*kan*	This study (De Lay & Cronan, 2008)
***S. flexneri* 2a**		

Table 3 (continued).

WT	2457T Wild Type, serotype 2a (AE014073.1)[a]	Walter Reed Army Institute of Research (Wei *et al*., 2003)
clsA	2457T *Δcls*::*kan* (AAP16748.1)	This study
clsB	2457T *ΔybhO*::*kan* (AAP16251.1)	This study
clsC	2457T *ΔymdC*::*kan* (AAP16548.1)	This study
clsAB	2457T *Δcls*::FRT, *ΔybhO*::*kan*	This study
clsAC	2457T *Δcls*::FRT, *ΔymdC*::*kan*	This study
clsBC	2457T *ΔymdC*::FRT, *ΔybhO*::*kan*	This study
clsABC	2457T *Δcls*::FRT, *ΔymdC*::FRT, *ΔybhO*::*kan*	This study
pbgA	2457T *ΔyejM190-586*::*kan* (AAP17611.1)	This study
icsA	2457T *icsA*::E2-Tn5 (AAL72293.1)	H. Marman
vpsC	2457T, *ΔvpsC*::*kan* (AAP18513.1)	This study (Carpenter *et al*., 2014)
rol	SA100, serotype 2a *Δrol*::*kan*	(Hong & Payne, 1997)

[a]Genome or loci accession number.

4. RNA Techniques

4.1 IN VITRO *S. FLEXNERI* RNA ISOLATION.

CR^+ colonies were grown overnight at 30°C in LB with aeration and then diluted 1:100 into LB+ 0.01% Sodium deoxycholate (DOC) and grown at 37°C with aeration to an OD_{650} of~ 0.7. Using RNA-Bee (Tel-Test, Inc.), RNA was harvested from the cells followed by DNas I (Life Technologies) treatment to remove genomic DNA.

4.2 IN VIVO *S. FLEXNERI* RNA ISOLATION.

Intracellular RNA was isolated by infecting semiconfluent Henle-407 monolayers with approximately 10^8 CFU grown to midlog in LB + 0.01% DOC. At 4 hours post-infection monolayers were treated with RNA-BEE and treated in an identical manner as described above.

4.3 AMPLIFICATION OF CDNA.

cDNA was generated using Superscript III reverse transcriptase (Life Technologies) with 2 μg of RNA as cDNA template.

4.4 QUANTITATIVE PCR.

Power SYBR Green (Life Technologies) chemistry was used to amplify and detect targets. All probes were designed using Primer Express software (Applied Biosystems). Primers used for qPCR are listed in Table 4, indicated by RT in their primer

name. cDNA was diluted 1:100 for detection by probes. Analysis was performed using an Applied Biosystems 7300 Real Time PCR system and software. Threshold cycle (C_T) values were normalized against those for *accD* and analysis was performed using the $\Delta\Delta C_T$ approach.

Table 4. Primers for quantitative PCR.

Primer	Sequence (5' to 3')
accD-RT-F	ATGGCGAAACTTGCAGAAAC
accD-RT-R	AAGCACTGATGTCGCTGATG
pbgA-RT-F	ATTCTGCTTTCGCTCGTCAT
pbgA-RT-R	CTGAAATGGCCGATAATGCT
clsA-RT-F	AGCAACGGGCTGAAGAAGTA
clsA-RT-R	AGGTTTTGGTGCAGACCTTG
clsB-RT-F	GGCGGTACTCAAAAACCTGA
clsB-RT-R	ACTGATCATTCAGGGCGAAC
clsC-RT-F	GCCGGATGCACAATAAAAGT
clsC-RT-R	GGCCTATTGCCATGACATCT

5. Cell Culture Techniques

5.1 Media and Growth conditions.

Henle cells (intestine 407; ATCC CCL-6), were cultured in minimal essential medium (MEM) (Gibco) containing: 10% (v/v) heat-inactivated fetal bovine serum (FBS) (Gibco); 10% (w/v) Bacto tryptone phosphate broth (Difco); 1X nonessential amino acids (Gibco); 2 mM glutamine. Colorectal cells (HT-29; ATCC HTB-38) were cultured in McCoy's 5A medium (Gibco) supplemented with 10% (v/v) heat-inactivated FBS (Invitrogen). Henle and HT-29 cells were incubated at 37°C with 95% air and 5% CO_2. Gentamicin was used at a final concentration of 40 μg/ml.

5.2 Plaque Assay.

Plaque assays were performed as previously described (Oaks *et al*., 1985). Briefly, bacteria were grown to an OD_{650} of ~ 0.5. Approximately 10^4 CFU of bacteria were added to a confluent monolayer of Henle cells in 35 mm, 6-well, polystyrene plates (Corning) and centrifuged for 10 min at 1,000 X *g*. Plates were incubated for 60 min, and the monolayers were washed 4 times with phosphate-buffered saline (PBS-D) (1.98 g KCl, 8 g NaCl, 0.02 g KH_2PO_4, 1.39 g K_2HPO_4). The media was then replaced with MEM containing gentamicin and 0.45% (w/v) glucose, and plates were then incubated for 24 hrs, after which the medium was replaced with MEM containing only gentamicin, and plates were incubated for an additional 48 hrs. Monolayers were washed with PBS-D and stained with Wright-Giemsa stain (Camco) for visualization.

5.3 INVASION ASSAY.

Invasion assays were performed as previously described (Hale & Formal, 1981). Briefly, bacteria were grown to an OD_{650} of ~ 0.5. Approximately 10^8 CFU of bacteria were added to a semi-confluent monolayer of Henle cells in 35 mm, 6-well, polystyrene plates (Corning) and centrifuged for 10 min at 1,000 X *g*. Plates were incubated for 30 min and monolayers were washed 4 times with PBS-D. The media was replaced with MEM containing gentamycin, and the plates were incubated for an additional 40 min. Monolayers were washed with PBS-D and stained with Wright-Giemsa stain (Camco). Monolayers were visualized using bright-field microscopy at 1,000 X magnification. Henle cells were scored positive for invasion if they contained 3 or more *S. flexneri* cells. A total of 300 Henle cells per well were counted.

5.4 INTRACELLULAR GROWTH RATES.

Intracellular growth rates were measured by growing bacteria in LB containing 0.1% DOC to an OD_{650} of ~ 0.5. Approximately 5 x 10^8 CFU of bacteria were added to a confluent monolayer of Henle cells in 22.1 mm, 12-well, polystyrene plates (Corning) and centrifuged for 10 min at 1,000 X *g*. Plates were then incubated for 30 min. Monolayers were then washed 4 times with PBS-D, and media was replaced with MEM containing gentamicin. Monolayers were washed with PBS-D after 60 min and 180 min, and lysed using 1.0% DOC. Lysates were diluted and plated on TSB agar, grown overnight at 37°C, and colonies were counted. The number of bacteria recovered at 60 min and 180 min post-infection were used to calculate the doubling time.

5.5 CELL-TO-CELL SPREAD.

The analysis was performed as previously described (Carpenter *et al*., 2014). Briefly, bacteria were grown to an OD_{650} of ~ 0.5. Approximately 10^7 CFU of bacteria were added to a confluent monolayer of Henle cells in 35 mm, 6-well, polystyrene plates (Corning) and centrifuged for 10 min at 1,000 X *g*. Plates were incubated for 30 min and the monolayers were then washed 4 times with PBS-D. The media was replaced with MEM containing gentamicin and the plates were incubated for an additional 4 hrs. Monolayers were washed with PBS-D and stained with Wright-Giemsa stain. Henle cells were scored positive for spread if they contained 3 or more *S. flexneri* cells and if adjacent Henle cells also contained 3 or more *S. flexneri* cells. 100 Henle cells per well were counted.

6. Fluorescence Microscopy Techniques

6.1 Size of Infected Foci.

The size of infection foci formed in plasma membrane-YFP-expressing HT-29 cells grown in McCoy's medium (Gibco, Life Technologies) and infected with the listed CFP-expressing *S. flexneri* strains was determined in a 96-well plate format (Corning, cat# 3904). After fixation, plates were imaged using the ImageXpress Micro imaging system (Molecular Devices) and image analysis for foci size determination was performed with the ImageXpress imaging software (Molecular Devices) as previously described (Dragoi & Agaisse, 2014).

6.2 Monitoring of Bacteria Dissemination.

Bacterial dissemination was monitored using time-lapse confocal microcopy. Plasma membrane-YFP-expressing HT-29 cells were grown in McCoy's medium in 8-well chambers (Lab-Tek II, cat# 155409, Thermo Fisher Scientific) at 37°C in 5% CO_2. Cells were infected with the listed CFP-expressing *S. flexneri* strains and imaged with a Leica DMI 8 spinning-disc confocal microscope driven by the iQ software (Andor). Z-stacks were captured 2 hours post-infection every 2 minutes for 6 hours. The corresponding movies were generated with the Imaris software (Bitplane).

6.3 Visualization of IcsA.

IcsA was visualized as previously described (Purdy *et al*., 2007). Briefly, bacteria were grown to mid-logarithmic phase and fixed in 4% (v/v) paraformaldehyde in PBS.

Cells were then labeled by indirect immunofluorescence, using rabbit polyclonal antibody against IcsA (Rabbit 35) diluted 1:100, provided by Edwin Oaks (Walter Reed Army Institute of Research), and a fluorescent isothiocyanate-conjugated goat anti-rabbit secondary antibody diluted 1:100 (Purdy *et al*., 2002).

6.4 POLAR TARGETING OF ICSA.

Polar targeting of IcsA was measured as previously described (Doyle *et al*., 2015b). Bacteria expressing p*icsA-gfp* were grown to mid-logarithmic phase and fixed in 4% (v/v) paraformaldehyde in PBS. Cells were then imaged using a GFP filter cube.

7. Lipid Techniques

7.1 Isolation of Inner and Outer Membranes.

Inner and outer membranes were isolated by pelleting mid-log bacteria at 13,000 X *g* for 10 min, resuspending in buffer containing 10mM Na_2HPO_4, and 5mM $MgSO_4$, sonicating to induce cell lysis, and centrifuging at 13,000 X *g* for 20 min to remove cell debris. The supernatant was then centrifuged at 135,000 X *g* for 40 min to isolate the total membranes. Total membranes were resuspended in 1.0% (w/v) Sarkosyl using a blunt needle and incubated at room temperature for 20 min. Following centrifugation at 135,000 X *g* for 40 min, the inner membrane remained in the supernatant while the outer membranes were pelleted. The pelleted outer membranes were resuspended in fresh 1.0% (w/v) Sarkosyl and used for downstream assays.

7.2 Isolation of Phospholipids.

Bacteria were grown in LB to an OD_{650} of ~ 0.5 (mid-log), or as indicated. Phospholipids were extracted according to the method of Bligh and Dyer (Bligh & Dyer, 1959).

7.3 Visualization of Phospholipids.

Phospholipids were spotted onto a Silica Gel 60 (Millipore) thin-layer chromatography (TLC) plate and separated by a chloroform-methanol-acetic acid (65:25:10, vol/vol) solvent system (Giles *et al*., 2011). Phospholipids were detected by spraying TLC plates with the Molybdenum Blue spray reagent (Sigma). The area of each

phospholipid species was quantified using ImageJ software (Schneider *et al*., 2012) to determine the percentage of each phospholipid in the sample.

7.4 DETECTION OF LIPOPOLYSACCHARIDES.

The assay was performed as previously described (Tsai & Frasch, 1982). Briefly, bacteria were grown at 37°C to OD_{650} ~ 0.5, and the equivalent of OD_{650}=1 was pelleted and resuspended in Laemmli SDS-PAGE sample buffer (Laemmli, 1970). Samples were then boiled for 10 min, cooled to room temperature, and treated with 25 μg proteinase K for 1 hour at 55°C. LPS was visualized by (4-12%) SDS-PAGE (Bolt Bis-Tris Plus, Invitrogen) and subsequent staining of the LPS with silver stain as follows; gels were fixed in 40% isopropanol and 5% acetic acid, oxidized with 0.7% periodic acid, stained with 20% silver nitrate, and developed using 50 μg/ml citric acid.

8. Protein Techniques

8.1 SDS-PAGE.

Samples were resuspended in Laemmli SDS sample buffer (5% β-mercapto-ethanol, 3% [wt/vol] SDS, 10% glycerol, 0.02 g bromophenol blue, 63 mM Tris-Cl, pH 6.8) (Laemmli, 1970), and boiled for 5 min. Samples were electrophoresed in quadruplicate (10%) SDS-PAGE gels for separation. Proteins were visualized by Coomassie brilliant blue staining and used to assess equal loading of samples for immunoblotting.

8.2 IMMUNOBLOTTING.

Proteins were transferred to a 0.45 μm pore size nitrocellulose membrane (GE Healthcare) and incubated with either rabbit polyclonal anti-IcsA antibody (Edwin Oaks, Walter Reed Army Institute of Research) diluted 1:10,000, rabbit polyclonal anti-SecA antibody (Donald Oliver, Wesleyan University) diluted 1:10,000, rabbit polyclonal anti-OmpA antibody (Donald Oliver, Wesleyan University) diluted 1:5,000, rabbit polyclonal anti-DegP (George Georgiou, The University of Texas at Austin) diluted 1:500, or mouse monoclonal anti-V5 antibody (Thermo Fisher Scientific) diluted 1:500. Proteins were detected using horseradish peroxidase-conjugated goat anti-rabbit antibody (diluted 1:5,000). Signal was detected by developing the blot with a Pierce ECL detection Kit (Thermo Fisher Scientific).

8.3 PURIFICATION OF ICSA.

Purification was performed as previously described (Leupold *et al*., 2017). *E. coli* cells BL21DE3 expressing p*icsA*-His or p*icsA*-His-Arg564Ala were sub-cultured 1:100 and grown in LB + ampicillin to mid-log phase at 37°C, induced with IPTG and grown for 5 hours at 25°C. Cells were then pelleted at 10,000 X *g* for 20 min at 4°C and washed with 150 mM NaCl. Bacterial pellets were stored at -80°C until protein purification.

Thawed pellets were resuspended in lysis buffer (50 mM HEPES pH 7, 300 mM NaCl, 10 mM imidazole pH 7, 1% Triton X-100, 10% Glycerol, 5 mM β-mercapto-ethanol and protease inhibitor [Roche]) and sonicated at 4°C. Lysates were then pelleted at 10,000 x *g* for 30 min at 4°C and the supernatant was added to a Ni-NTA Affinity Resin column (EMD Milipore) and incubated for 2 hours at 4°C. Using a gravity flow column, th resin was washed (50 mM HEPES pH 7, 300 mM NaCl, 30 mM imidazole pH 7, 1% Triton X-100, and 5 mM β-mercapto-ethanol) with 50 column volumes, and proteins were eluted (50 mM HEPES pH 7, 300 mM NaCl, 250 mM imidazole, and 5 mM β-mercapto-ethanol) in 2 column volumes.

Elution fractions were analyzed by SDS-PAGE, and fractions containing protein were digested with TEV protease by adding 2% (w/w) to each elution fraction and incubating overnight at 4°C. Fractions were then pooled and concentrated using Amicon Ultra-15 30NMWL columns (EMD Millipore). Protein was buffer exchanged into storage buffer (50 mM HEPES pH 7, 150 mM NaCl) to a final concentration of 10 mg/ml and stored at 4°C.

8.4 IcsA Co-Sedimentation.

Dried glycerolphospholipids (Cardiolipin, phosphatidylglycerol and phosphatidylethanolamine [Avanti Polar Lipids]) were resuspended in IcsA protein storage buffer (50 mM HEPES pH 7, 150 mM NaCl) to a final concentration of 1 mg/ml. Lipids were sonicated and vortexed to form a suspension. 10 μg of protein was incubated with 1 mg glycerolphospholipids for 1 hour at 37°C. The reactions were then centrifuged at 14,000 x *g* for 30 min, and supernatants and pellets were collected and Tricholoracetic Acid (TCA) precipitated. Precipitated fractions were resuspended in Laemmli SDS sample buffer for SDS-PAGE analysis. Proteins were visualized by Coomassie staining. The area of each protein species was quantified using ImageJ software (Schneider *et al*., 2012) to determine the percentage of each protein in the sample.

8.5 Trypsin Cleavage of IcsA.

Trypsin cleavage of IcsA was performed as previously described (Besingi & Clark, 2015). Briefly, bacteria were grown to mid-logarithmic phase and equivalent cell numbers were divided (~$8x10^8$ cells), pelleted and were resuspended in Protease buffer (50 mM Tris pH 8.8, 7.5 mM $CaCl_2$). Prior to digestion, one sample was sonicated to induce lysis. Trypsin (Sigma) was diluted to a final concentration of 10, 5, and 1 μg/ml and allowed to digest cell samples for 1 hour at 25°C. Samples were pelleted and resuspended in Laemmli SDS sample buffer for SDS-PAGE analysis. Proteins were visualized by Coomassie staining, and western blot analysis using anti-IcsA, anti-OmpA, and anti-DegP antibodies.

III. RESULTS

1. Chapter 1: Characterization of Cardiolipin Synthesis and Transport[1]

Cardiolipin is a large anionic phospholipid that localizes to the inner leaflet at the poles of Gram-negative bacteria. To characterize the mechanism *S. flexneri* uses to synthesize and transport cardiolipin, a series of mutants were constructed that disrupted one of the three putative inner membrane cardiolipin synthases, *clsA*, *clsB*, and *clsC* (Figure 4), or the transporter, *pbgA* (Figure 6).

1.1 *S. FLEXNERI* CARDIOLIPIN IS SYNTHESIZED PRIMARILY BY CLSA.

In *E. coli*, cardiolipin is synthesized by *clsA*, *clsB*, and *clsC*, which either condense two phosphatidylglycerol molecules (*clsA* and *clsB*)) (Guo & Tropp, 2000; Pluschke *et al*., 1978) or condense phosphatidylglycerol and phosphatidylethanolamine molecules (*clsC*) (Tan *et al*., 2012), to produce cardiolipin (Figure 4). *S. flexneri*'s genome contains the genes *cls*, *ybhO*, and *ymdC* with homology to *E. coli clsA*, *clsB*, and *clsC*, respectively, which we have re-named to match the *E. coli* gene nomenclature. To determine the contribution of each predicted *S. flexneri* cardiolipin synthase, we constructed individual deletion mutants and examined their phospholipid composition using the Bligh-Dyer phospholipid isolation technique and subsequent TLC separation for visualization (Bligh & Dyer, 1959). When compared to WT, deletion of *clsA* resulted in the loss of detectable cardiolipin and a small increase in the level of

[1] Portions of this work have been previously published in mBio (**Rossi, R. M., Yum, L., Agaisse, H. & Payne, S. M. (2017).** Cardiolipin Synthesis and Outer Membrane Localization Are Required for *Shigella flexneri* Virulence. *mBio* **8**, e01199–17.) by the American Society for Microbiology. R. M. Rossi designed and carried out all experiment herein with assistance from co-authors.

phosphatidylglycerol in the membrane of *S. flexneri* during exponential growth (Figure 9). The synthesis of cardiolipin was restored by introducing wild type *clsA* on a plasmid. Complementation with *clsA* also reduced PG levels to wild type. In contrast, the deletion of *clsB* and *clsC* had no detectable effect on cardiolipin levels under these conditions. This suggests ClsA is the major cardiolipin synthase enzyme of *S. flexneri*.

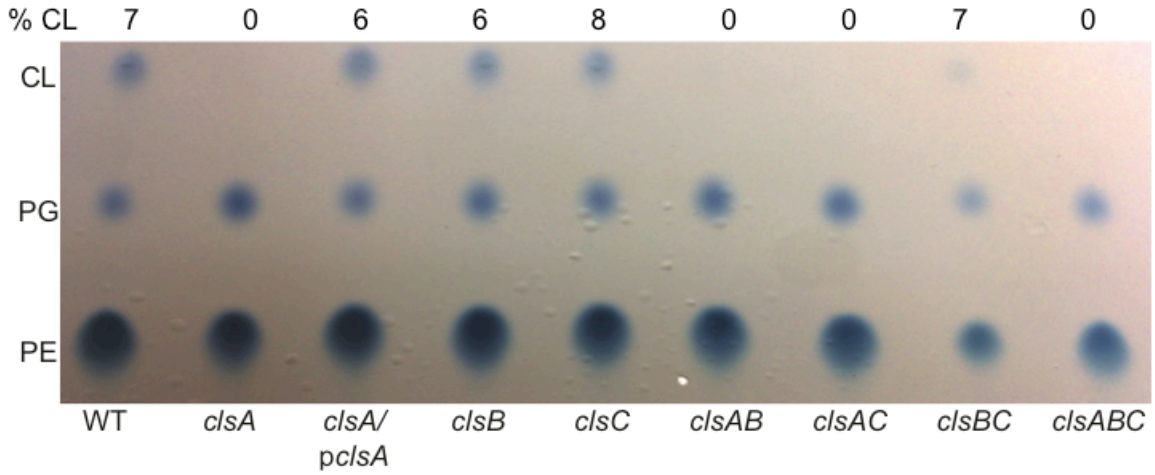

Figure 9. ClsA is the major cardiolipin synthase of *S. flexneri*.

TLC analysis of total *S. flexneri* membrane phospholipids of the wild type (WT) and cardiolipin synthesis mutants. Bacteria were grown to mid-log phase, and phospholipids were extracted and separated by TLC. The percentage of cardiolipin in the sample is indicted above each lane. Phospholipids were visualized using molybdenum blue spray (Sigma). The phospholipids include phosphatidylethanolamine (PE) phosphatidylglycerol (PG), and cardiolipin (CL). p*clsA*, plasmid expressing *clsA*. Figure taken from (Rossi *et al*., 2017).

1.2 ClsC CONTRIBUTES TO *S. FLEXNERI* CARDIOLIPIN SYNTHESIS IN STATIONARY PHASE.

Previous studies have shown that *E. coli* produces higher levels of cardiolipin during growth in stationary phase (Hiraoka *et al*., 1993). To determine if *S. flexneri* also increases the amount of cardiolipin during stationary phase, we extracted and separated phospholipids from *S. flexneri* grown to stationary phase. We found the proportion of cardiolipin in *S. flexneri*'s membrane slightly increased in stationary phase (Figure 10). Interestingly, the *clsA* mutant showed detectable levels of cardiolipin during stationary phase growth, indicating an additional cardiolipin synthase(s) is active. To determine which cardiolipin synthase is active during stationary growth, we assessed the phospholipid levels in the cardiolipin synthase double mutants and found that the *clsA clsC* double mutant did not contain cardiolipin within its membrane during stationary phase growth, indicating that ClsC is an active cardiolipin synthase during stationary phase.

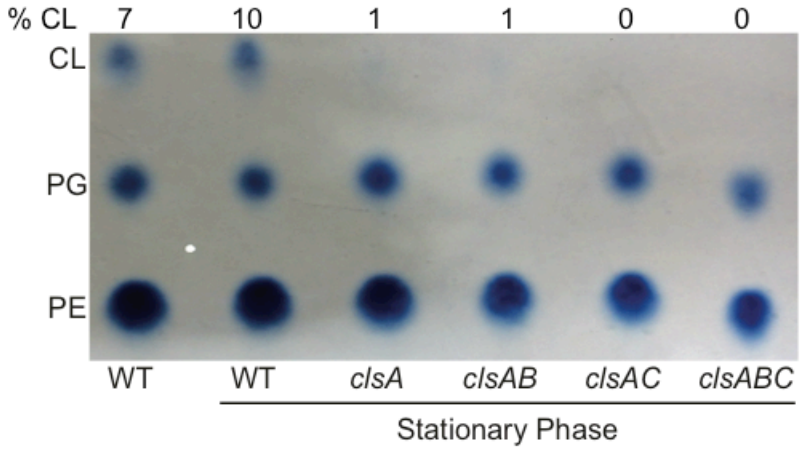

Figure 10. Cardiolipin synthesis increases during stationary phase growth.

Bacteria were grown into stationary phase (OD_{650} of ~2.0); phospholipids were then extracted and separated by TLC. The percentages of cardiolipin in the sample are indicated above each lane. Phospholipids were visualized using molybdenum blue spray (Sigma). The phospholipids include phosphatidylethanolamine (PE), phosphatidylglycerol (PG), and cardiolipin (CL). Figure taken from (Rossi *et al*., 2017).

1.3 CARDIOLIPIN LOCALIZES TO BOTH THE INNER AND OUTER MEMBRANES OF *S. FLEXNERI*.

In Gram-negative bacteria, phospholipids are the major lipid components of the entire inner membrane and the inner leaflet of outer membrane. To determine if cardiolipin is found in both the inner and outer membranes of *S. flexneri*, we fractionated the inner and outer membranes using Sarkosyl solubilization and assessed their phospholipid composition by thin layer chromatography. Cardiolipin was found in both the inner and outer membranes of *S. flexneri* (Figure 11A), and the phospholipid distribution between the inner and outer membranes was similar. To confirm clean separation of the inner and outer membrane, samples of cell fractions were analysed by SDS-PAGE and Western blotting; the inner membrane protein SecA was not detected in the outer membrane fractions, and the outer membrane protein OmpA was only found in the outer membrane fractions (Figure 11B).

In addition, we fractionated the inner and outer membrane of the *clsA* mutant and found that the inner and outer phospholipid distributions look similar; however, both had increased levels of phosphatidylglycerol and no detectable cardiolipin, when compared to WT. The wild type levels of cardiolipin and PG and localization of cardiolipin to both the inner and outer membranes, was restored by complementation with *clsA* on a plasmid. This suggests that *S. flexneri* maintains equivalent phospholipid distributions between its inner and outer membranes.

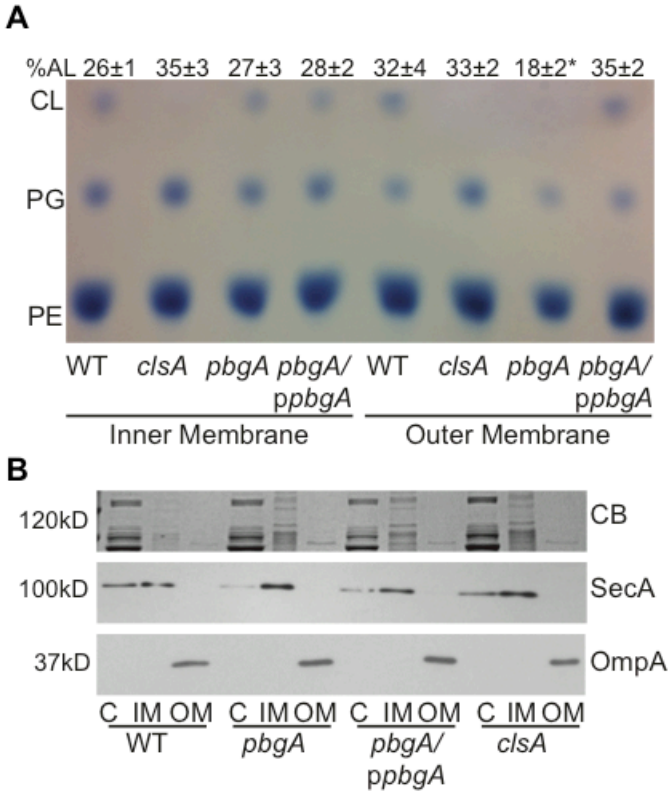

Figure 11. ***S. flexneri*** **requires** ***pbgA*** **for localization of cardiolipin to its outer membrane.**

TLC analysis of *S. flexneri* inner and outer membrane phospholipids. (A) Inner and outer membrane composition analysis of pbgA and clsA mutants. Bacteria were grown to mid-log phase, and bacterial membranes were separated by solubilization in Sarkosyl. The phospholipids were then extracted, spotted for separation by TLC, and visualized using molybdenum blue spray reagent (Sigma). The phospholipids include phosphatidylglycerol (PG), phosphatidylethanolamine (PE), and cardiolipin (CL). The percentage of anionic phospholipids (AL) in the sample is indicated above each lane, and the means and standard deviations of three experiments are shown. The value that is significantly different ($P < 0.05$) from the value for the outer membrane of the wild type by Student's t test is indicated by an asterisk. (B) Confirmation of clean inner and outer

membrane fractions. Bacteria were grown to mid-log phase, and the bacterial membranes were separated by solubilization using Sarkosyl. Proteins were resolved by (10%) SDS-PAGE and stained with Coomassie blue (CB) or immunoblotted using either polyclonal anti-SecA or polyclonal anti-OmpA. The molecular masses (in kilodaltons) of molecular mass markers are shown to the left of the gels. ppbgA, plasmid expressing pbgA; C, cytoplasm; IM, inner membrane; OM, outer membrane. Figure taken from (Rossi *et al*., 2017).

1.4 CARDIOLIPIN IS TRANSPORTED TO *S. FLEXNERI* OUTER MEMBRANE BY PBGA.

In *S*. Typhimurium, activation of PhoPQ induces the expression of *pbgA*, which increases outer membrane integrity by transporting cardiolipin to the outer membrane (Figure 6) (Dalebroux *et al*., 2015). Complete deletion of *pbgA* in *E. coli* and *S*. Typhimurium is lethal; however, deletion of the C-terminal periplasmic portion reduced cardiolipin transport to the outer membrane (De Lay & Cronan, 2008). Therefore, we made a similar deletion of the C-terminus of the *S. flexneri pbgA* homolog (*yejM*) to determine the effects of eliminating cardiolipin from the outer membrane. Membrane fractionation and analysis of the phospholipids confirmed that the mutant lacked cardiolipin in the outer membrane. As expected, the phospholipid composition of the inner membrane of the *pbgA* mutant looked identical to the WT (Figure 11A). Interestingly, unlike the *clsA* mutant, which had increased amounts of PG within its membrane in the absence of cardiolipin, the *pbgA* outer membrane did not have increased PG levels. Complementation with full-length *pbgA* on a plasmid restored cardiolipin in the outer membrane. In addition, we determined that the whole cell phospholipid profile was not disrupted in the *pbgA* mutant when compared to wild type (WT) (Figure 12). Together, this suggests that *S. flexneri* PbgA is responsible for transporting cardiolipin and PG to the outer membrane.

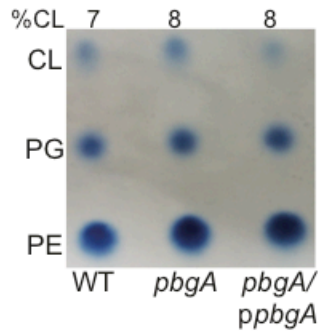

Figure 12. *pbgA* mutant has wild-type cardiolipin levels.

TLC analysis of total *S. flexneri* membrane phospholipids of the *pbgA* mutant. Bacteria were grown to mid-log phase, and phospholipids were extracted and separated by TLC. Phospholipids were visualized using molybdenum blue spray (Sigma). The percentage of cardiolipin in the sample is indicated above each lane. The phospholipids include phosphatidylethanolamine (PE) phosphatidylglycerol (PG), and cardiolipin (CL).

1.5 *S. FLEXNERI CLSA* IS HIGHLY EXPRESSED IN VITRO.

Because *S. flexneri* shares a large proportion of genetic homology with *E. coli*, and the genetic landscapes surrounding all cardiolipin synthases are conserved, it is possible that the contribution to cardiolipin synthesis by ClsB and ClsC in *S. flexneri* is reduced because they are not expressed. During exponential growth, *S. flexneri clsA* was induced approximately 100-fold compared to *E. coli clsA*, and *clsC* was induced approximately 5-fold (Figure 13). However, *S. flexneri clsB* expression mimicked *E. coli*, suggesting the inactivity of ClsB is unrelated to its expression. The high expression of *clsA* could contribute to the dominant effect ClsA has on cardiolipin synthesis.

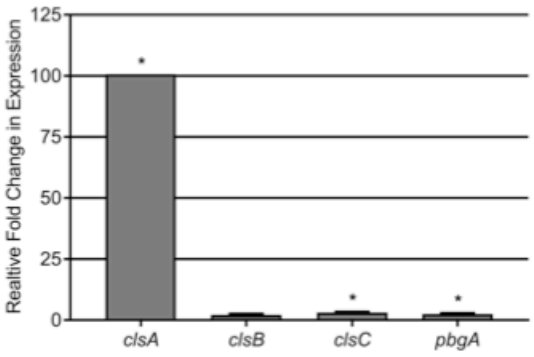

Figure 13. mRNA levels of *S. flexneri clsA* are highly expressed compared to *E. coli.*

Expression of *clsA* is increased in *S. flexneri* as determined by quantitative real-time PCR. Bacteria were subcultured 1:100 into LB and grown to mid-log phase and RNA from approximatly10^8CFU was isolated and used to determine message levels. Threshold cycle (C_T) values were normalized against those for *accD*, analysis was performed using the $\Delta\Delta C_T$ approach and are shown relative to the *E. coli* level set to 1. (*) *P*-value of <0.05 compared to the *E. coli* expression levels (by Student's t-test).

1.6 *S. FLEXNERI PBGA* IS HIGHLY EXPRESSED IN VITRO.

The genetic landscapes surrounding the encoded cardiolipin transporter *pbgA* are conserved between *S. flexneri* and *E. coli*; however, during exponential growth, *S. flexneri pbgA* was induced approximately 5-fold compared to *E. coli pbgA* (Figure 13). The higher expression of *pbgA* in *S. flexneri* could contribute to an increased amount of cardiolipin in the outer membrane of *S. flexneri* compared to *E. coli*. An *E. coli* mutation in *pbgA* results in a reduction of outer membrane integrity (Hirvas *et al*., 1997). The increase in cardiolipin could increase the outer membrane integrity of *S. flexneri,* allowing them to survive more harsh conditions than *E. coli*.

1.7 CHAPTER 1 CONCLUSION.

Cardiolipin is a large anionic phospholipid, which makes up approximately 7% of *S. flexneri*'s membrane phospholipids. Cardiolipin specifically localizes to the inner leaflet of the bacterial poles (Oliver *et al*., 2014). This is because cardiolipin has a small glycerol head group and a large acyl region with 4 chains, giving the overall structure of cardiolipin a conical shape. Bacteria lacking cardiolipin do not have altered cell morphology, supporting the model that the conical shape of cardiolipin does not dictate the negative curvature of the poles, but that its localization at the poles is a consequence of its shape. Cardiolipin localizes to bacterial poles via diffusion because of its natural tendency to destabilize planar membranes.

Analysis of *S. flexneri* phospholipids revealed that cardiolipin makes up approximately 7% of its total phospholipids and is found in equal amounts between the inner and outer membrane. We determined that ClsA is the major cardiolipin synthase of *S. flexneri* and the level of phosphatidylglycerol increases in both the inner and outer

membrane in the absence of cardiolipin, which maintains the overall anionic phospholipid levels (Figure 14). In addition, we determined that PbgA transports cardiolipin and phosphatidylglycerol to the *S. flexneri* outer membrane, but has no effect on the inner membrane phospholipids.

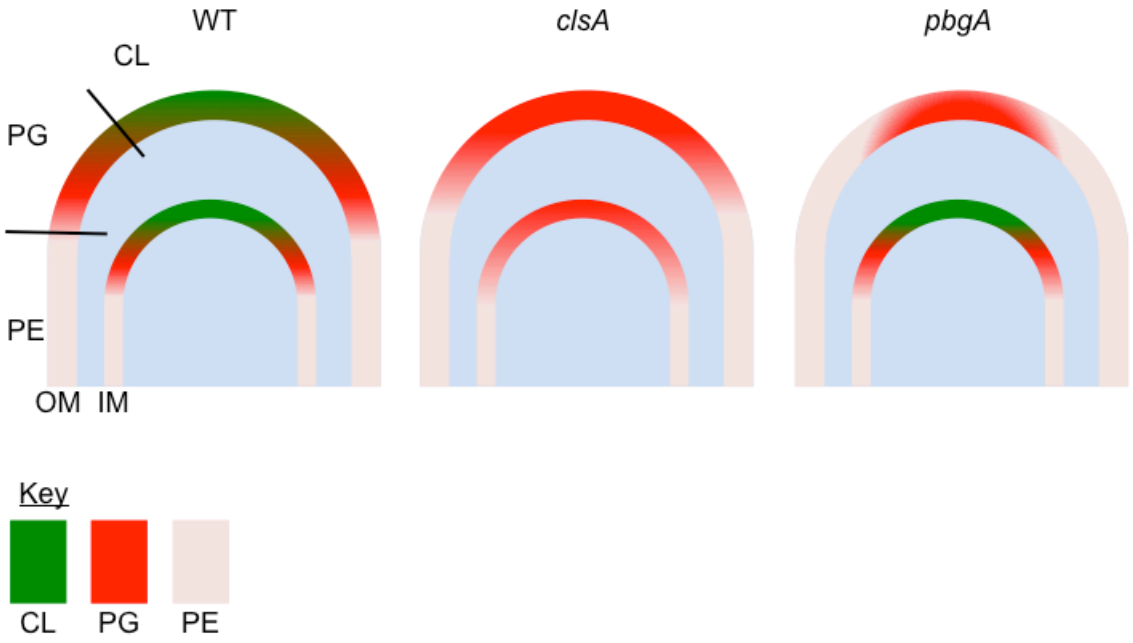

Figure 14. Schematic of proposed phospholipid localization in WT, *clsA*, and *pbgA* mutants.

clsA and *pbgA* have different membrane composition compared to the wild type. (WT) the inner and outer membranes are identical. Cardiolipin localizes to the bacterial pole, phosphatidylglycerol localizes adjacent to cardiolipin, and phosphatidylglycerol localizes to non-polar regions. (*clsA*) the inner and outer membrane are identical; however, they do not contain cardiolipin and have increased phosphatidylglycerol levels. (*pbgA*) the inner membrane is identical to WT, while the outer membrane does not contain cardiolipin and has reduced phosphatidylglycerol. Phospholipids include; phosphatidylethanolamine (PE) phosphatidylglycerol (PG), and cardiolipin (CL).

2. Chapter 2: Role of Cardiolipin in Pathogenesis[2]

To cause disease, *S. flexneri* must efficiently invade colonic epithelial cells and spread intercellularly to neighboring cells. Previous studies have shown that outer membrane integrity, mediated by asymmetric distribution of phospholipids and Lipid A structure, is required by *S. flexneri* during intercellular spread (Carpenter *et al*., 2014); however, the role of specific phospholipids in *S. flexneri* pathogenesis had not been determined.

Much remains unknown regarding cardiolipin's role in bacterial membranes and this is likely for two reasons. First, most enteric bacteria have three cardiolipin synthases, and all three must be inactivated in order to eliminate cardiolipin from the bacterial membrane; most studies to date have only been performed on bacteria with reduced cardiolipin levels. Second, phosphatidylglycerol, which is similar to cardiolipin in that it also has a glycerol head group and is an anionic phospholipid, can interact with proteins in a similar manner and compensate for the lack of cardiolipin within the bacterial membrane. Thus, bacteria lacking cardiolipin do not display an *in vitro* growth phenotype. These concerns have complicated studying cardiolipin's role in bacterial pathogenesis. Here we assay the *S. flexneri* cardiolipin synthesis and transport mutants' ability to form plaques in cultured epithelial monolayers to assess for virulence (Oaks *et al*., 1985).

[2] Portions of this work have been previously published in mBio (**Rossi, R. M., Yum, L., Agaisse, H. & Payne, S. M. (2017).** Cardiolipin Synthesis and Outer Membrane Localization Are Required for *Shigella flexneri* Virulence. *mBio* **8**, e01199–17.) by the American Society for Microbiology. R. M. Rossi designed and carried out all experiment herein with assistance from co-authors.

2.1 CARDIOLIPIN SYNTHESIS BY CLSA IS REQUIRED FOR PLAQUE FORMATION.

To determine the role of cardiolipin in *S. flexneri* pathogenesis, we performed plaque assays (Oaks *et al*., 1985) with each of the cardiolipin synthesis mutants. *S. flexneri* is an intracellular pathogen, and plaque formation requires invasion of the Henle cell monolayer, intracellular replication, and spread to the adjacent cells. After 72 hours, the *clsA* mutant formed pinpoint plaques compared to WT. Plaque formation was complemented by *clsA* on a plasmid (Figure 15). This suggests cardiolipin synthesis by ClsA is required for wild type plaque formation.

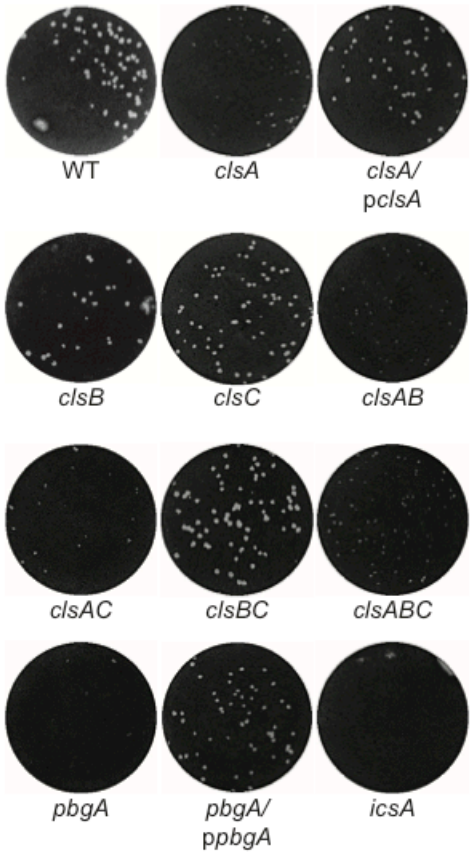

Figure 15. *clsA* and *pbgA* are required for *S. flexneri* plaque formation.

Confluent monolayers of Henle cells were infected with approximately 10^6 CFU of bacteria. Monolayers were stained and photographed after 72 h to visualize plaque formation. Figure taken from (Rossi *et al*., 2017).

2.2 EXPRESSION OF *CLSB* AND *CLSC* INCREASE DURING INTRACELLULAR GROWTH.

Because ClsC contributed to cardiolipin synthesis in stationary phase (Figure 10), it was possible that *clsB* or *clsC* is expressed in the intracellular environment and contributed to sufficient cardiolipin to support formation of very small plaques. Analysis of intracellular mRNA levels revealed that both *clsB* and *clsC* were induced approximately 10-fold in the intracellular bacteria (Figure 16), while *clsA* was unchanged. Therefore, cardiolipin synthesis by ClsB and ClsC may contribute to plaque formation.

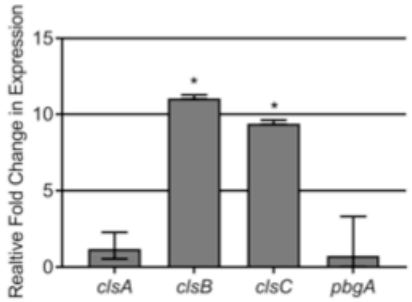

Figure 16. *clsB* and *clsC* expression increase in the intracellular environment.

Quantification of cardiolipin synthases and transport genes, determined using quantitative real-time PCR. Bacteria were sub-cultured 1:100 into LB + 0.01% DOC and grown to mid-log phase. Cultures were divided, and RNA from approximately 10^8 CFU was isolated and used to determine extracellular message levels, and semi-confluent Henle-407 monolayers were infected with the remaining approximately 10^8 CFU. RNA was isolated 4 hours post infection, by lysing infected monolayer with RNA-Bee, and used to determine intracellular mRNA levels. Threshold cycle (C_T) values were normalized against those for *accD*. Analysis was performed using the $\Delta\Delta C_T$ approach and values are shown relative to the extracellular level set to 1. (*) *P*-value of <0.05

compared to extracellular expression levels (by Student's t-test). Figure taken from (Rossi *et al*., 2017).

2.3 ClsB and ClsC do not contribute to cardiolipin synthesis during plaque formation.

Since expression of *clsB* and *clsC* increase in the intracellular environment, it is possible that they may contribute to cardiolipin synthsis during plaqe formation. However; mutation in *clsB* and *clsC* did not affect *S. flexneri* plaque formation (Figure 15), indicating that that ClsB and ClsC do not synthesize sufficient cardiolipin in intracellular bacteria to compensate fully for the loss of *clsA*.

2.4 Transport of cardiolipin to the outer membrane is required for plaque formation.

Next, we wanted to determine if cardiolipin is required in the outer membrane of *S. flexneri* for plaque formation, therefore we test the *pbgA* mutant that does not have cardiolipin within it outer membrane. The *pbgA* mutant was unable to form plaques compared to WT (Figure 15), and displayed a similar plaque phenotype to an *icsA* mutant that is unable to spread intercellularly. Plaque formation by the *pbgA* mutant was restored by full-length *pbgA* on a plasmid. This indicates that cardiolipin within the outer membrane is critical for plaque formation. The *clsA* and *pbgA* mutants were further characterized to determine more precisely the roles of cardiolipin in *S. flexneri* virulence.

2.5 Cardiolipin is not required for *S. flexneri* maintenance of membrane integrity.

Previous studies have show that a disruption in the outer membrane integrity inhibits *S. flexneri* plaque formation (Carpenter *et al*., 2014), and *pbgA* is required to maintain membrane integrity in other Gram-negative bacteria (Dalebroux *et al*., 2015; Hirvas *et al*., 1997). To determine whether the defect in plaque formation by *clsA* and *pbgA* mutants is the result of reduced outer membrane integrity to due to the lack of

cardiolipin, we assessed the mutants for increased sensitivity to Deoxycholate (DOC), an ionic bile acid that disrupts the membrane. The *clsA* and *pbgA* mutants grew similar to the wild type, with an average doubling time of 41 min, both in the absence (Figure 17A) and presence (Figure 17B) of DOC. In contrast, the *vpsC* mutant, which has compromised outer membrane stability (Carpenter *et al*., 2014), was inhibited in the presence of DOC.

Interestingly, in the presence of DOC, the expression of *clsA, clsB*, *clsC,* and *pbgA* all increase (Figure 18), suggesting there may be regulation of cardiolipin synthesis and transport under membrane stress conditions similar to *S*. Typhimurium (Dalebroux *et al*., 2014). However, because membrane integrity remains, this suggest that cardiolipin within the outer membrane of *S. flexneri* is not playing a structural role in the integrity of the outer membrane of *S. flexneri*.

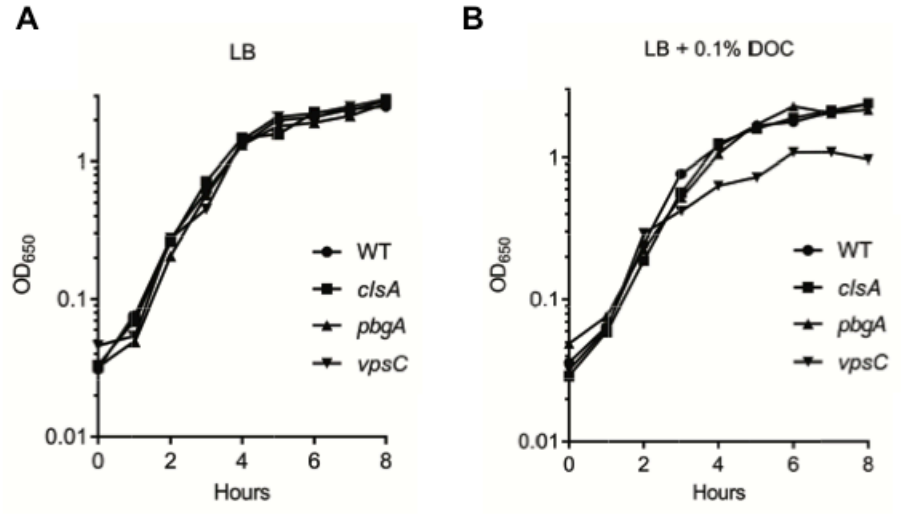

Figure 17. Cardiolipin synthesis and outer membrane transport are not required for growth in the presence of DOC.

clsA and *pbgA* mutant strains do not exhibit growth sensitivity to DOC. (A) Bacteria were subcultured 1:100 into LB (A), or LB containing 0.1% DOC (B), and grown into stationary phase. Data shown is representative of three biological replicates.

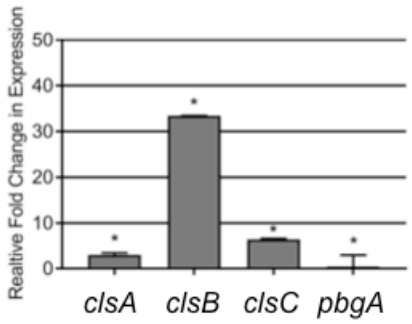

Figure 18. Cardiolipin synthase and transport gene expression increases in the presence of DOC.

As determined by quantitative real-time PCR. Bacteria were subcultured 1:100 into LB and grown to mid-log phase and RNA from approximately 10^8 CFU was isolated and used to determine message levels. Threshold cycle (C_T) values were normalized against those for *accD*. Analysis was performed using the $\Delta\Delta C_T$ approach and values are shown relative to the extracellular level set to 1. (*) *P*-value of <0.05 compared to the growth in LB expression levels (by Student's t-test).

2.6 CARDIOLIPIN IS NOT REQUIRED FOR CELLULAR INVASION.

The initial stage of *S. flexneri* virulence requires the bacteria to invade colonic epithelial cells (Labrec *et al*., 1964; Oliver *et al*., 2014). A requirement for cardiolipin in invasion would give fewer or no plaques. To determine if cardiolipin is required for invasion, we compared the *clsA* and *pbgA* mutants with wild type and found that neither mutant had a significant defect in invasion compared to the wild type parental strain (Figure 19). Infection rates were determined for cells grown in the presence and absence of DOC, since previous work (Pope *et al*., 1995) had shown that DOC increased virulence protein secretion and infectivity of wild type *Shigella*.

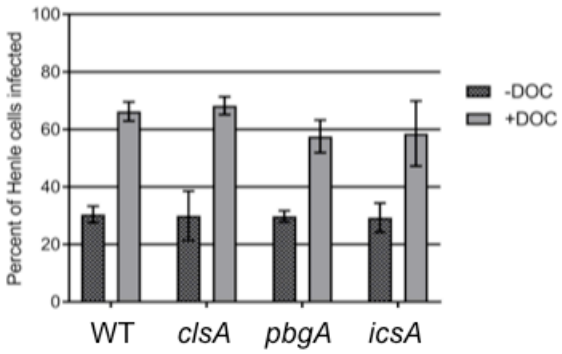

Figure 19. Cardiolipin synthesis and outer membrane transport are not required for *S. flexneri* invasion.

Invasion rates of *clsA* and *pbgA* mutants. Percent of Henle cells that contained 3 or more intracellular bacteria. The data represent mean values of three biological replicates with standard deviation. Compared to wild type, none of the mutants had a statistical difference in invasion or intracellular doubling time by Student's t-test, *P*-value <0.05.

2.7 CARDIOLIPIN IS NOT REQUIRED FOR INTRACELLULAR GROWTH.

Once inside the epithelial cell the bacteria rapidly replicate (Sansonetti *et al*., 1986). A requirement for cardiolipin in this process could explain reduced plaque formation. To assess intracellular replication, we isolated intracellular bacteria at 60 and 180 min post-infection and determined their doubling time. We found that compared to WT, neither the *clsA* nor the *pbgA* mutant had a significant defect in intracellular replication (Figure 20). Together, these data indicate cardiolipin is not required in the inner or outer membrane of *S. flexneri* for Henle cell invasion and intracellular replication during the first 3 hours of infection.

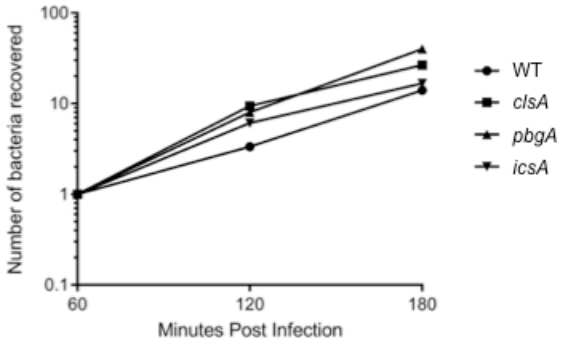

Figure 20. *S. flexneri pbgA* and *clsA* mutants replicate similar to WT intracellularly.

Doubling time of bacteria during the first three hours of intracellular growth. The numbers of intracellular bacteria were determined by lysing infected Henle monolayers, followed by plating of the lysate dilutions. Cell counter were normalized to the 1 hour time point. Data represent the mean values of three biological replicates and standard deviations. Compared to wild type, none of the mutants had a statistical or intracellular doubling time by Student's t-test, *P*-value <0.05.

2.8 CARDIOLIPIN IS REQUIRED FOR CELLULAR DISSEMINATION.

The lack of an effect of cardiolipin on invasion and intracellular replication suggested that the plaque defect was due to lack of cell-to-cell spread of the bacteria. To determine the role of cardiolipin in *S. flexneri* intercellular spread, we determined the percentage of primary Henle cell infections resulting in spread to neighboring cells after 4 hours, using a cell-to-cell spread assay (Carpenter *et al*., 2014). Primary infected Henle cells were identified as cells containing large numbers of bacteria, indicating intracellular replication (Figure 21A). Infective centers were scored positive for spread if one or more neighboring cells had 3 or more intracellular bacteria. After 4 hours, wild type *S. flexneri* had spread from > 80% of the initially infected cells to neighboring cells (Figure 21B). The *clsA* and *pbgA* mutants, however, had significant defects in intercellular spread, with a spread rate of only 20 and 24%, respectively. This rate mimicked the rate of an *icsA* mutant that cannot spread (Bernardini *et al*., 1989). The intercellular spread defect of both the *clsA* and *pbgA* mutants could be complemented by the addition of the full-length protein expressed from a plasmid. This suggests the defect in plaque formation of both the *clsA* and *pbgA* mutants is their inability to spread intercellularly.

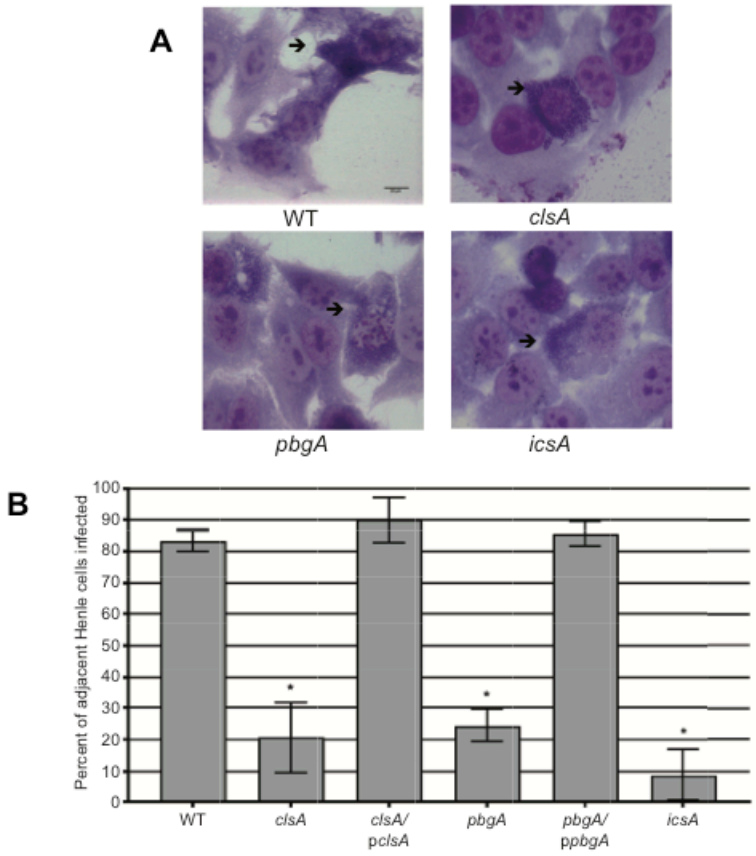

Figure 21. Cardiolipin is required for *S. flexneri* intercellular spread.

Semiconfluent Henle monolayers were infected with approximately 10^7 CFU of bacteria. Monolayers were stained after 4 hr, and intercellular spread was visualized by bright-field microscopy. (A) Micrographs of intercellular spread by WT *S. flexneri* and *clsA*, *pbgA*, and *icsA* mutants. Black arrows point to primary infected Henle cells. (B) Graphical representation of *S. flexneri* intercellular spread. One hundred infected Henle cells were counted positive for spread if the surrounding Henle cells were also infected. Values are means and standard deviations (error bars) for three biological replicates. Values that are significantly different ($P < 0.05$) from the value for the wild type by Student's t test are indicated by an asterisk. Figure taken from (Rossi *et al*., 2017).

2.9 *CLSA* IS REQUIRED FOR FOCI FORMATION IN HT-29 CELLS.

Intercellular spread of *S. flexneri* is a dynamic, multi-step process (Agaisse, 2016); it requires the bacteria to polymerize host actin to move and penetrate neighboring cells (Philpott *et al*., 2000), re-activate their T3SS to eject effector proteins into neighboring cell cytoplasm (Campbell-Valois *et al*., 2014), and resolve the membrane protrusions into neighboring cells (Kuehl *et al*., 2014). To specifically determine at which point during intercellular spread the *clsA* and *pbgA* mutants have a defect, we used infection of HT-29 intestinal cells, which allowed us to employ time-lapse confocal microscopy to monitor cell-to-cell spread over an extended period of time (Dragoi & Agaisse, 2014). First, using computer-assisted image analysis, cell-to-cell spread was quantified by measuring the area of the infected foci in cellular monolayers.

Although the *clsA* mutant showed a defect in spread within 4 hours in Henle cells, the decrease in foci area in HT-29 cells was not detected until 8-16 hours of infection. At 16 hours, the *clsA* mutant showed a significant decrease in foci area compared to the WT (Figure 22A), and this defect in intercellular spread was complemented with full-length *clsA* on a plasmid (Figure 22B).

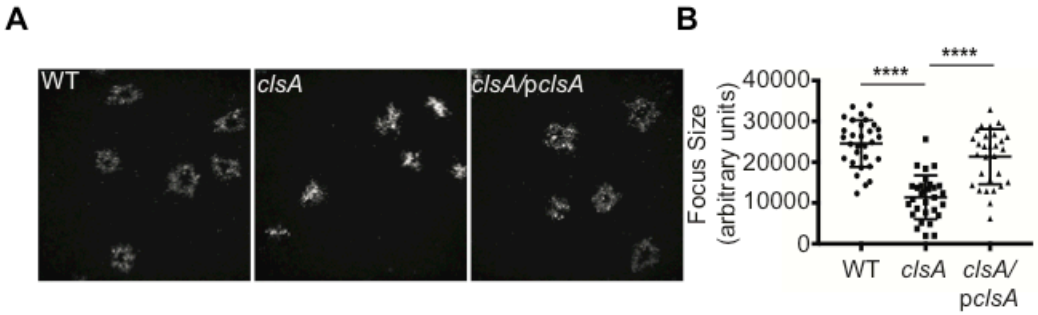

Figure 22. *clsA* has reduced dissemination in HT-29 cells after 16 hours.

(A) Low-magnification image of WT and *clsA* mutant foci and small plaque formation at 16 h to determine their size. (B) Quantification of WT and *clsA* mutant foci and small plaque formation at 16 h. Values that are significantly different ($P < 0.0001$) by Student's t test are indicated by a bar and four asterisks. Figure taken from (Rossi *et al*., 2017).

2.10 CARDIOLIPIN SYNTHESIS IS REQUIRED FOR PROPER INTRACELLULAR DIVISION OF *S. FLEXNERI*.

Using the HT-29 intestinal cell line model, we analyzed the timing of cell-to-cell spread of the *clsA* mutant by time-lapse confocal microscopy (Kuehl *et al*., 2014). HT-29 cell monolayers expressing plasma membrane-targeted yellow florescence protein (YFP) were infected with *S. flexneri* expressing IPTG-inducible cyan fluoresces protein (CFP), and individual bacteria were tracked. The wild-type strain showed rapid cell division, motility and spread to adjacent cells (Rossi *et al*., 2017). The *clsA* mutant (Rossi *et al*., 2017) appeared similar to the wild type at the early time points. It was motile in the initially infected cell and had normal intracellular growth for the first 6 hours (Figure 23).

However, after an extended period of time (6 hrs), independent of the bacteria being in the cytoplasm of the primary infected cell or neighboring cells, the *clsA* mutant was no longer able to divide properly and formed filaments (Figure 24). Filamenting bacteria were non-motile, which inhibited further spread, or they formed protrusions that were unable to form vacuoles and retracted back into the cell. Thus, cardiolipin is required in the membrane of *S. flexneri* for proper cell division after extended intracellular growth.

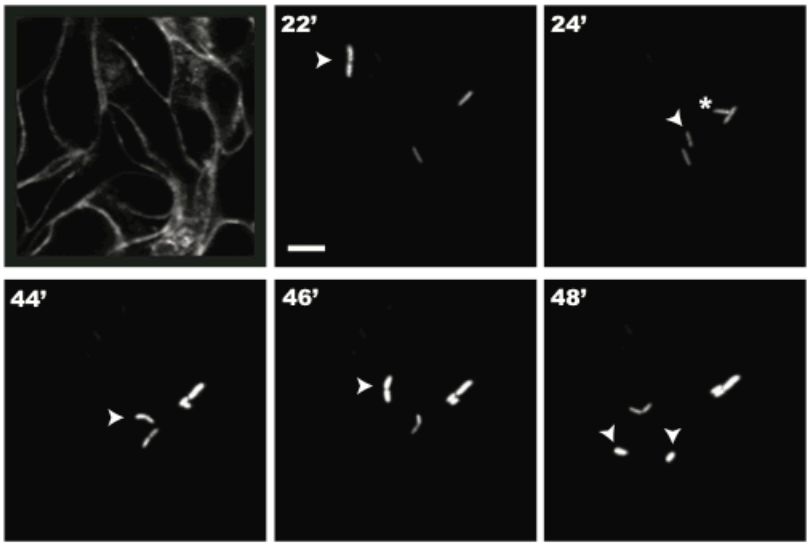

Figure 23. *clsA* behaves like wild type early during intracellular growth.

Basal Z-section slice of the HT-29 monolayer footprint prior to infection and early infection tracking of a normal growing bacterium. Arrowhead tracking of a bacterium about to divide at 22 min (22'), which gives rise to two bacteria shown at 24 min, indicated by an arrowhead and asterisk. The arrowhead was tracked until the next cell division shown at 48 min. Bars = 5 μm. Figure taken from (Rossi *et al*., 2017).

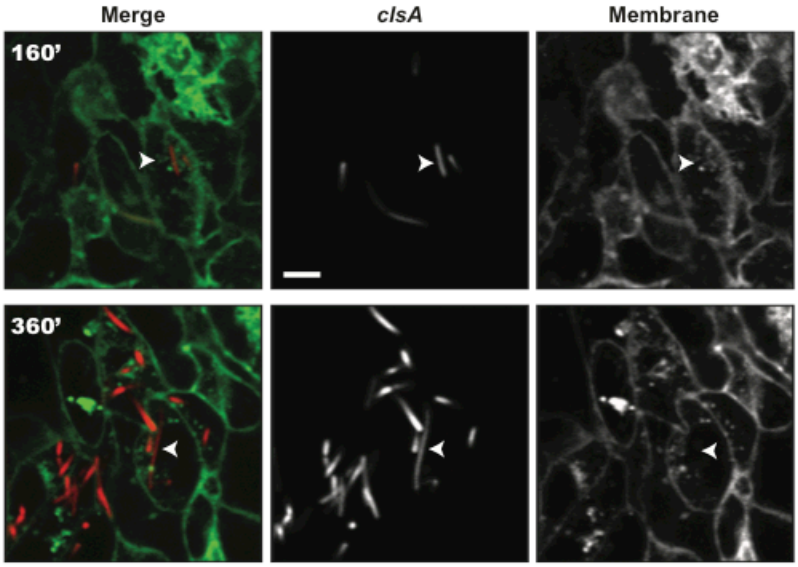

Figure 24. *clsA* is required for intracellular division late during intracellular growth.

Basal Z-section slice of the HT-29 monolayer footprint tracking of an abnormally growing bacterium. Late infection tracking of one cytosolic filamenting bacterium at 160 and 360 min. Bars = 5 μm. Figure taken from (Rossi *et al*., 2017).

2.11 INNER MEMBRANE CARDIOLIPIN IS REQUIRED FOR PROPER CELL DIVISION DURING INTRACELLULAR GROWTH.

Unlike the *clsA* mutant, after 8 hours, the *pbgA* mutant showed a significant decrease in the area of intercellular spread in HT-29 cells compared to WT (Figure 25A), and this impairment in intercellular spread was complemented with full-length *pbgA* on a plasmid (Figure 25B). This indicates that outer membrane cardiolipin is required for *S. flexneri* intercellular spread early in infection. The delay in a detectable spread defect for the *clsA* mutant compared to the *pbgA* mutant may be due to partial compensation by the increased PG in the outer membrane of the *clsA* mutant.

To more precisely define whether the defect in intracellular replication in the cardiolipin synthesis mutant (*clsA*) was due to lack of cardiolipin in the inner or the outer membrane, we also performed time-lapse microscopy on the *pbgA* mutant, which has cardiolipin in the inner, but not the outer, membrane (Rossi *et al*., 2017). Unlike the *clsA* mutant, the *pbgA* mutant grew normally within the cytoplasm of HT-29 cells, indicating that cardiolipin is needed in the inner membrane for maintaining wild type replication in the intracellular environment. However, the *pbgA* mutant was non-motile inside the eukaryotic cell and did not spread intercellularly. Thus, cardiolipin in the outer membrane is needed for intracellular motility.

For comparison, the *vpsC* mutant, which has altered phospholipids and lipid A modifications in the outer membrane (Carpenter *et al*., 2014), was analyzed (Rossi *et al*., 2017). The *vpsC* mutant had an intracellular infection phenotype that was distinct from either of the cardiolipin mutants. It replicated normally and was motile, but the motility was less than wild type, and there was no spread to adjacent cells.

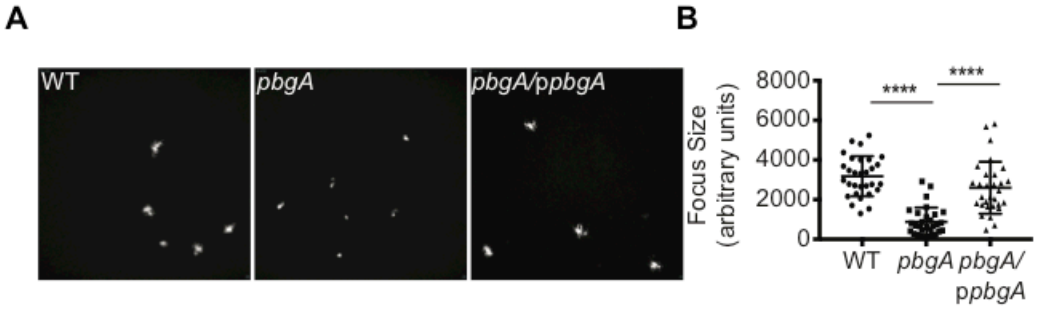

Figure 25. *pbgA* has reduced dissemination in HT-29 cells after 8 hours.

(A) Low-magnification image of WT and *pbgA* mutant focus formation at 8 h to determine their size. (B) Quantification of WT and *pbgA* mutant focus formation at 8 h. Values that are significantly different (P 0.0001) by Student's t test are indicated by a bar and four asterisks. Figure taken from (Rossi *et al*., 2017).

2.12 OUTER MEMBRANE ANIONIC PHOSPHOLIPIDS ARE REQUIRED FOR ICSA LOCALIZATION.

Since the *pbgA* mutant was non-motile within the intracellular environment, it suggests that it has a defect in the localization or export of IcsA. To determine if cardiolipin within the outer membrane is required for IcsA localization, we used indirect immunofluorescence directed against IcsA to visualize surface IcsA localization of *S. flexneri* grown *in vitro* (Purdy *et al*., 2007). When compared to WT, the *pbgA* mutant displayed no polar localization of IcsA (Figure 26), and had a low amount of IcsA detectable across its entire outer surface. Unipolar localization of IcsA was restored with full-length *pbgA* on a plasmid. For comparison, the *icsA* mutant had no detectable IcsA on its surface. This suggests that the lack of cardiolipin within the outer membrane of the *pbgA* mutant inhibits unipolar IcsA localization.

Since the *clsA* mutant was motile within the cytoplasm of HT-29 cells, we predicted that IcsA could still be localized to the bacterial pole. We found that in the *clsA* mutant (Figure 26), IcsA was localized to the poles; however, the amount of IcsA was reduced when compared to WT.

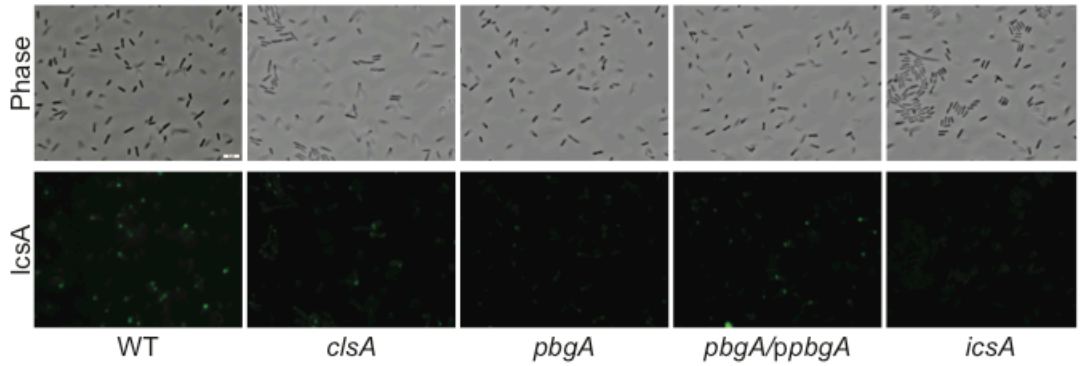

Figure 26. *pbgA* is required for unipolar IcsA localization.

Surface localization of polar IcsA, visualized by indirect immunofluorescence. Bacterial cultures were gown to mid-log phase (visualized by phase contrast microscopy), and IcsA was observed by indirect immunofluorescence (visualized by FITC). All images were captured with an exposure time of 1.5 s and processed in an identical manner. Bar = 5 μm. Figure taken from (Rossi *et al*., 2017).

2.13 CHAPTER 2 CONCLUSION

To date, roles of cardiolipin in bacterial pathogenesis have been identified in two pathogens, *S*. Typhimurium (Dalebroux *et al*., 2015) and *Moraxella catarrhalis* (Buskirk & Lafontaine, 2014). In *S*. Typhimurium cardiolipin is required in the outer membrane to provide membrane integrity. Increased expression of *pbgA* and remodeling of the outer membrane occurs in response to PhoPQ signaling during *Salmonella* infection, *Salmonella*, like *Shigella*, is an intracellular pathogen; however, *Salmonella* resides within phagosomes of macrophages, which may represent a more stressful environment than the cytoplasm. Since *S. flexneri* lacking cardiolipin does not have reduced membrane integrity when grown in the presence of DOC, and does not have an *in vivo* growth defect, it is unlikely that the role of cardiolipin in *S. flexneri* pathogenesis is maintenance of *S. flexneri* membrane integrity.

In *Moraxella catarrhalis*, cardiolipin is required for proper bacterial attachment to human epithelial cells (Buskirk & Lafontaine, 2014). It is hypothesized that cardiolipin is required for the localization or display of adhesion proteins. This may represent a similar function to cardiolipin's role in *S. flexneri*, where cardiolipin in the outer membrane is important for the localization of IcsA.

In the absence of cardiolipin, phosphatidylglycerol localizes to the bacterial pole and can interact with polar proteins, in the same, but less efficient manner as cardiolipin. We predict that in cardiolipin's absence in *S. flexneri*, other anionic phospholipids, such as phosphatidylglycerol, can help localize IcsA to the pole; however, this localization is not as specific or as efficient as when cardiolipin is present. This model is supported by the phenotype of a *pbgA* mutant, in which the absence of cardiolipin and an overall decrease in outer membrane anionic phospholipids resulted in a dispersed localization

pattern of IcsA on the surface of *S. flexneri* and a more severe phenotype in the spread and motility assays.

The loss of cardiolipin from the outer membrane without compensation by increased PG affects plaque formation by preventing IcsA localization. The effects of loss of cardiolipin from the inner membrane are less clear. The *clsA* mutant replicates normally in vitro and has no obvious defect early in infection of epithelial cells. However, longer exposure to the intracellular environment results in aberrant cell division and loss of motility. Studies in *E. coli* have shown that MinD, which is required for normal cell division, and osmotic stress proteins associate with cardiolipin in the inner membrane. Similar effects of cardiolipin on localization of inner membrane proteins in *S. flexneri* could cause the growth defects seen in the host cell cytoplasm.

Since the *pbgA* mutant maintains wild type levels of cardiolipin within the inner membrane, it suggests inner membrane cardiolipin is required for intracellular division (Figure 27), while the *clsA* mutant outer membrane has increased phosphatidylglycerol to compensate for the lack of cardiolipin, suggesting outer membrane anionic phospholipids are required for movement (Figure 27).

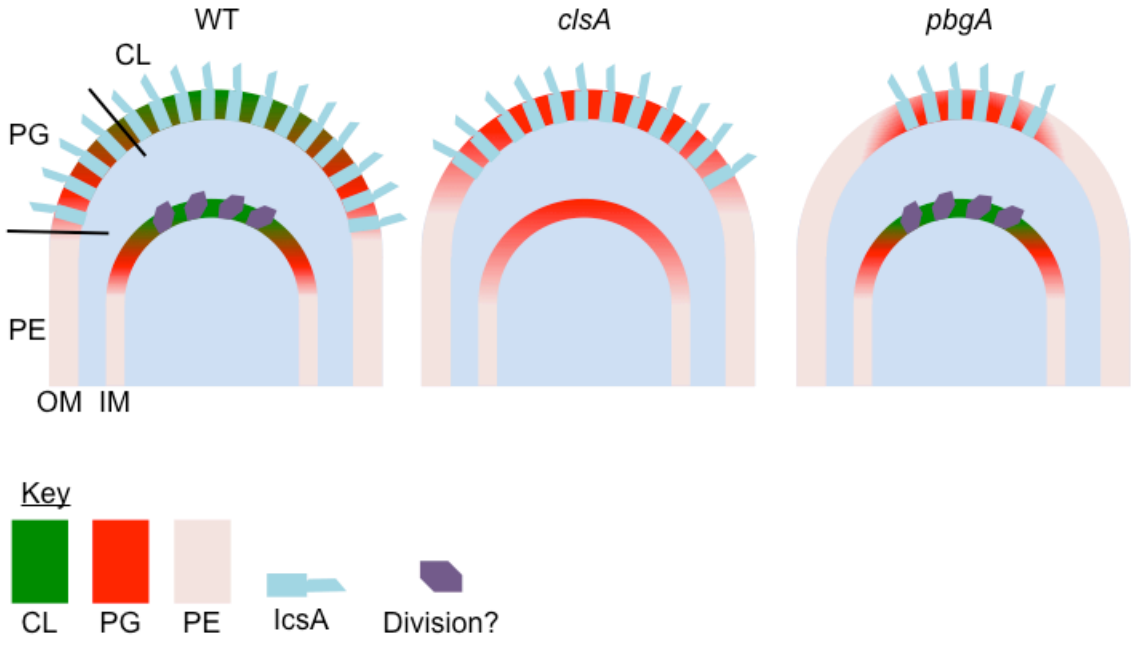

Figure 27. Schematic of outer and inner membrane localizing *S. flexneri* virulence proteins.

(WT) IcsA localizes to cardiolipin and PG in the outer membrane, and an unknown intracellular division protein localizes with cardiolipin in the inner membrane. (*clsA*) Most IcsA localizes with PG in the outer membrane, reducing intracellular movement. An unknown intracellular division protein does not have cardiolipin to localize to in the inner membrane, inhibiting intracellular division. (*pbgA*) IcsA does not have cardiolipin or PG to localize to in the outer membrane, inhibiting intracellular movement. An unknown intracellular division protein localizes with cardiolipin in the inner membrane. Phospholipids include; phosphatidylethanolamine (PE) phosphatidylglycerol (PG), and cardiolipin (CL).

3. Chapter 3: Interaction of Cardiolipin and IcsA[3]

Unipolar localization of *S. flexneri* virulence protein, IcsA, provides the mechanism for intracellular mobility through the polymerization of host actin, which is required for intercellular spread. *S. flexneri* IcsA is a member of the auto-transporter protein family, where its C-terminus functions as a beta-barrel in the outer membrane, and its N-terminal domain is fed through the barrel to expose the N-WASP recruitment domain on the surface of the bacteria. The direct mechanism by which IcsA localizes to the bacterial pole remains unknown. Here we examine the role of cardiolipin in polar targeting of IcsA.

3.1 Role of cardiolipin in IcsA localization is independent of Lipopolysaccharide structure.

Mis-localization of IcsA by the loss of outer membrane cardiolipin in the *clsA* and *pbgA* mutants could be an indirect. The one current model for *S. flexneri* IcsA polar localization suggests localization is directed by outer membrane O-antigen chain length synthesis (Doyle *et al*., 2015a). To determine whether the absence of cardiolipin disrupts O-antigen synthasis of *S. flexneri*, we compared the LPS of *clsA* and *pbgA* mutants to the wild type and to a previously characterized *rol* LPS mutant (Hong & Payne, 1997) by gel electrophoresis (Figure 28). The *clsA* and *pbgA* mutants did not have any detectable differences in LPS chain lengths when compared to WT. This suggests that the role of cardiolipin in *S. flexneri* IcsA localization is independent of O-antigen chain length.

[3] Portions of this work have been previously published in mBio (**Rossi, R. M., Yum, L., Agaisse, H. & Payne, S. M. (2017).** Cardiolipin Synthesis and Outer Membrane Localization Are Required for *Shigella flexneri* Virulence. *mBio* **8**, e01199–17.) by the American Society for Microbiology. R. M. Rossi designed and carried out all experiment herein with assistance from co-authors.

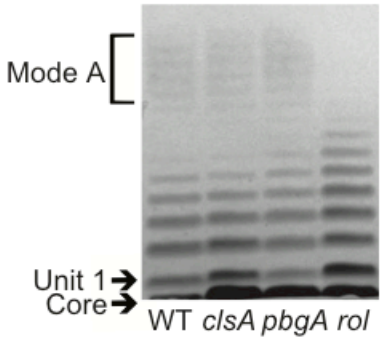

Figure 28. Cardiolipin is not required to maintain LPS structure.

LPS structure of *clsA* and *pbgA* mutants are similar to the wild type. Bacteria were grown to mid-log phase. LPS was extracted, resolved by (4 to 12%) SDS-PAGE, and visualized by silver staining. Figure taken from (Rossi *et al*., 2017).

3.2 CARDIOLIPIN IS NOT REQUIRED FOR ICSA TRANSPORT TO THE OUTER MEMBRANE

Although the anionic lipids cardiolipin and phosphatidylglycerol are known to be capable of localizing membrane proteins, the disruption in localization of IcsA could be indirect. This disruption in localization of IcsA could be a result of inefficient export of IcsA to the outer membrane (Purdy *et al*., 2002). To determine whether cardiolipin plays a role in efficient transport of IcsA to the outer membrane, we fractionated the inner and outer membranes of *S. flexneri* and examined the IcsA levels in each membrane using immunoblot analysis. We found that both the *clsA* and *pbgA* mutants had WT levels of IcsA within their outer membrane (Figure 29), indicating that cardiolipin is not necessary for IcsA export to the *S. flexneri* outer membrane or its stability in the membrane.

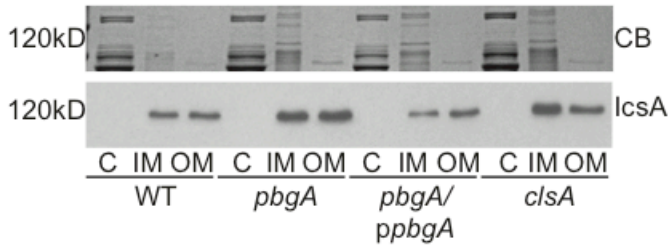

Figure 29. Cardiolipin is not required to maintain outer membrane IcsA levels.

Outer membrane IcsA levels. Bacteria were grown to mid-log phase. The membranes were fractionated using Sarkosyl membrane solubilization, resolved by (10%) SDS-PAGE, stained by Coomassie blue (CB) (Same gel pictured in Figure 11), and immunoblotted using polyclonal anti-IcsA antisera. C, cytoplasm; IM, inner membrane; OM, outer membrane. Figure taken from (Rossi *et al*., 2017).

3.3 OUTER MEMBRANE CARDIOLIPIN IS NOT REQUIRED FOR ICSA PASSENGER DOMAIN AUTO-TRANSPORT.

Upon reaching the outer membrane, the IcsA beta-barrel is first inserted into the outer membrane, and auto-transport of the IcsA passenger domain follows (Figure 6). However, we don't know if auto-transport follows immediately or only when IcsA is at the bacterial pole. It is possible that cardiolipin targets periplasmic IcsA directly to the outer membrane pole for beta-barrel insertion and subsequent transport of the N-terminal domain, and in the absence of cardiolipin insertion and transport is non-directed resulting in a more circumferential IcsA pattern. Alternatively, the periplasmic IcsA beta-barrel can be inserted anywhere in the outer membrane but N-terminal transport of IcsA can only occur when it interacts with cardiolipin, and in the absence of cardiolipin there is a reduced amount of N-terminal extracellular exposed IcsA. Since the IcsA antibody is against the passenger domain, visualization of polar IcsA only showed surface exposed IcsA (Figure 26).

To differentiate between these mechanisms, we analyzed the amount of surface exposed IcsA passenger domain in the *clsA* and *pbgA* mutants. Using extracellular trypsin protease, we can measure the amount of surface exposed peptides, which are sensitive to protease digestion, compared to transmembrane and periplasmic proteins that are not surfaced exposed (Besingi & Clark, 2015). Sonication followed by digestion with trypsin resulted in the complete degradation of *S. flexneri* IcsA passenger domain (Figure 30), and IcsA levels were restored in a dose dependent manner in the absence of sonication. Periplasmic DegP levels were only disrupted in the presence of sonication, and outer membrane OmpA levels were undisturbed, suggesting trypsin is only cleaving surface protein peptides.

When compared to the wild type, both the *clsA* and *pbgA* mutant had similar amounts of surface exposed IcsA (Figure 30). This suggests that outer membrane cardiolipin is not required for passenger domain auto-transport, but outer membrane cardiolipin is required to direct the cPT domain to the bacterial pole for beta-barrel insertion and subsequent auto-transport.

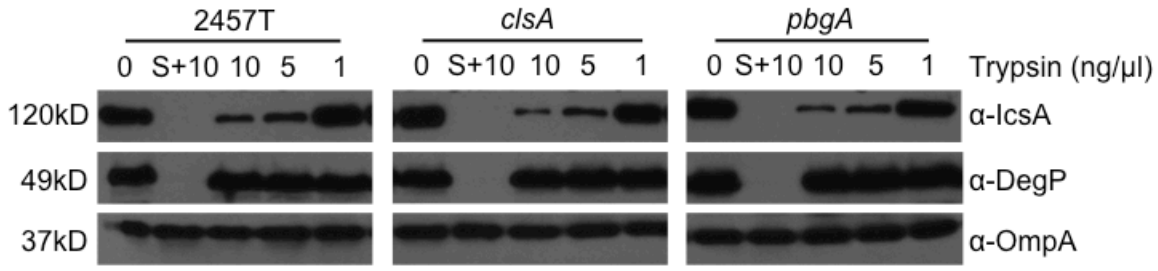

Figure 30. *clsA* and *pbgA* mutants have wild type levels of surface exposed IcsA.

Western blot analysis of IcsA, DegP and OmpA levels in the wild type, *clsA* and *pbgA* mutants after trypsin exposure. Bacterial cells were grown to mid-log, sonicated (S) and exposed to varying concentrations of trypsin. Samples were run on (12%) SDS-PAGE and immunoblotted using either polyclonal anti-IcsA, anti-DegP, or anti-OmpA antisera.

3.4 CARDIOLIPIN IS REQUIRED FOR POLAR TARGETING OF ICSA.

Directing of polar fluorescence to the bacterial pole by the IcsA cPT domain has been observed in other Gram-negative bacteria (Charles *et al*., 2001; Janakiraman *et al*., 2009), and this polar targeting is independent of secretion to the outer membrane. This suggests a conserved characteristic between all Gram-negative bacterial inner and outer membrane inner leaflets at the poles affect polar targeting of the cPT domain. Since cardiolipin is conserved between the inner leaflets of the Gram-negative bacterial membrane, we hypothesize cardiolipin may be directing polar targeting of IcsA via the cPT domain.

To determine if cardiolipin directs IcsA polar targeting via the cPT domain we constructed a fluorescent fusion protein of GFP to the cPT domain of IcsA and examined polar GFP in the *clsA* mutant (Figure 31A). When compared to the wild type and *pbgA* mutants, which have cardiolipin within their inner membrane, the *clsA* had reduced polar targeting of GFP (Figure 31B) suggesting cardiolipin directs polar targeting of IcsA via the cPT domain.

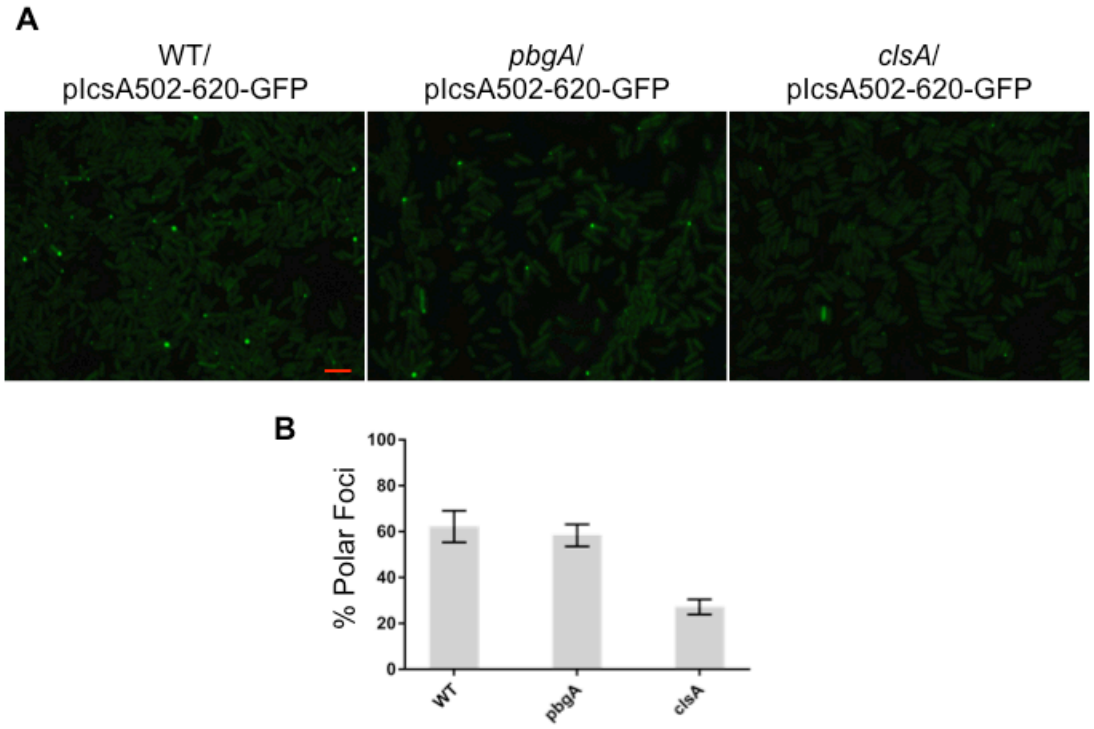

Figure 31. cPT polar targeting is disrupted in the *clsA* mutant.

IcsA502-620-GFP fusions expressed in the WT, *clsA* and *pbgA* mutants. (A) Bacterial cultures were grown to mid-log phase and IcsA polar targeting was observed by GFP fluorescence. (B) Quantification of polar foci frequency (n=200). All images were captured with an exposure time of 0.5 s and processed in an identical manner. Bar = 5 μm.

3.6 IcsA PASSENGER DOMAIN DIRECTLY INTERACTS WITH CARDIOLIPIN

In the inner mitochondrial matrix, lysine residues on the surface of Drp1 interact with the glycerol head group of cardiolipin, helping it localize with cardiolipin. It is possible that positively charged residues on the surface of the polar targeting (PT) domain identified in the N-terminal region of IcsA help IcsA localize with cardiolipin. Alternatively, cardiolipin could indirectly localize IcsA by interacting with the positively charged residues of other proteins known to aid in its localization and activity. For example, IcsA chaperone or secretion proteins may interact with cardiolipin to direct insertion of IcsA into the outer membrane at the poles. These interactions would promote polar localization of IcsA to allow directed movement by actin polymerization at the bacterial surface.

To determine if the interaction between the IcsA cPT domain and cardiolipin is direct, we purified the IcsA passenger domain (Leupold *et al*., 2017) and assessed its ability to interact with phospholipids using protein-lipid co-sedimentation assays. After protein-lipid incubation, if the protein is able to interact with the respective phospholipid, the protein will co-sediment with the lipid following centrifugation (Zhao & Lappalainen, 2012). In the absence of phospholipid, IcsA is found in the supernatant fraction (Figure 32A), while incubation with positively charged phosphatidylethanolamine resulted in a small fraction of the protein in the pellet, suggesting IcsA binds poorly to phosphatidylethanolamine.

A significant shift in IcsA found in the pellet fraction is observed when it is co-incubated with negatively charged phosphatidylglycerol (Figure 32A), and this interaction can be disrupted with the addition of Mg^{2+}. However, the most significant protein-lipid interaction is observed when IcsA is co-incubated with negatively charged

cardiolipin (Figure 32A). Together, this suggests that the IcsA passenger domain is a lipid binding protein with a preference for negatively charged anionic phospholipids.

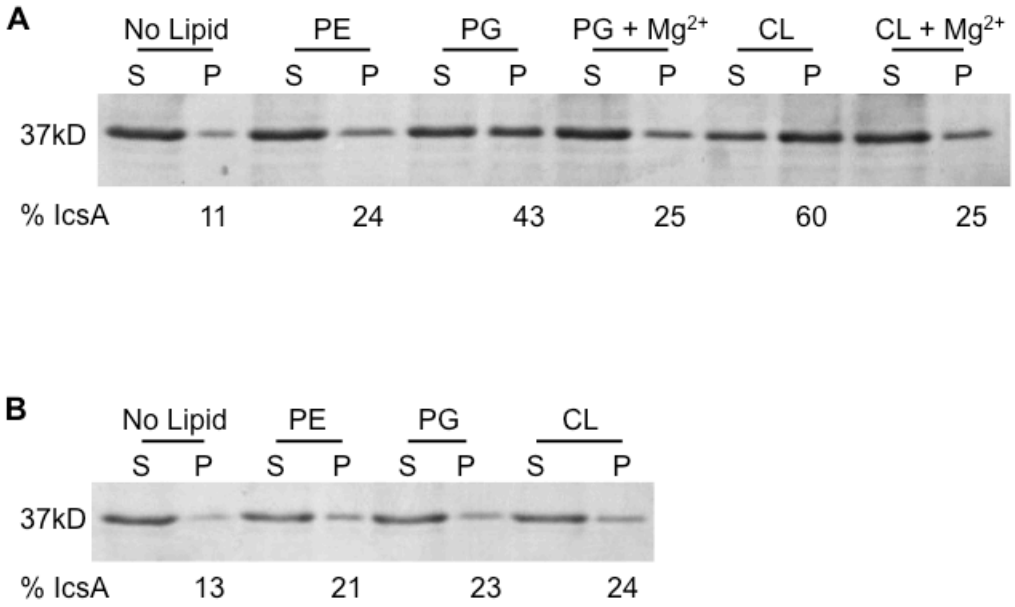

Figure 32. IcsA cPT domain directly interacts with cardiolipin.

Protein-lipid co-sedimentation assay of the IcsA (A) wild type, and (B) Arg564Ala mutant. Proteins were incubated with phospholipids and centrifuged. Supernatant (S) and Pellet (P) fractions were isolated, and then analyzed by SDS-PAGE and subsequent Coomassie staining. Phospholipids include; phosphatidylethanolamine (PE) phosphatidylglycerol (PG), and cardiolipin (CL).

3.7 IcsA Amino acid Arg546 in the cPT domain is important for polar targeting.

Previous studies have identified two intrinsic domains that direct IcsA to the bacterial pole (Charles *et al*., 2001; Doyle *et al*., 2015b), nPT and cPT (Figure 8). Mutational (Doyle *et al*., 2015b) and structural (Leupold *et al*., 2017) studies have elucidated a specific amino acid residue that directs the cPT domain to the bacterial pole. This residue, IcsA-Arg564, is surface exposed and does not play a role in maintaining IcsA structure. An amino acid substitution to an Ala maintains total protein levels and outer membrane IcsA levels (Table 5.); however, it reduces the amount of polar IcsA and *S. flexneri* plaquing efficiency. This suggests this residue is required for direct polar targeting of IcsA.

Comparing the phenotypes of *S. flexneri clsA* and *pbgA* mutants to *icsA* Arg564Ala identified a similarity between the *clsA* and *icsA* Arg564Ala mutation (Table 5.). Both mutations reduce *S. flexneri* plaquing efficiency, and this is a direct result of reduced surface polar IcsA, independent of total and outer membrane IcsA levels.

Table 5. Comparisons of *icsA* Arg564Ala, *clsA*, and *pbgA*.

Mutant/ Characterization	***icsA* Arg564Ala**	***clsA***	***pbgA***
Plaque	Pinpoint	Pinpoint	None
Total IcsA	WT	WT	WT
Outer Membrane IcsA	WT	WT	WT
Surface Polar IcsA	Reduced	Reduced	Pinpoint

Adapted from Doyle *et al*. (2015), Leupold *et al*. (2017), and Rossi *et al*. (2017).

3.8 IcsA cPT domain Arg564 is required for cardiolipin interaction.

Cardiolipin has previously been shown to directly interact with positively charged protein residues (Duncan *et al*., 2016). Therefore, we hypothesized that the IcsA passenger domain was interacting with cardiolipin via the positively charged Arg564 residue, shown previously to be required for polar targeting of the IcsA cPT domain (Doyle *et al*., 2015b). We purified the IcsA passenger domain containing the amino acid substitute Arg564Ala, and determined its ability to interact with cardiolipin. When compared to the wild type IcsA, IcsA-Arg564Ala was significantly reduced in its ability to interact with the anionic phospholipids phosphatidylglycerol and cardiolipin (Figure 32B). Together, this suggests that the IcsA passenger domain interacts with cardiolipin at amino acid Arg564, within the cPT domain.

3.9 Chapter 3 Conclusion

A number of different mechanisms by which *S. flexneri* localizes IcsA to the bacterial pole had been proposed but there was not conclusive evidence for any of theses. Here we show that cardiolipin direct IcsA polar localization independent of O-antigen chain length, export to the bacterial outer membrane, and exposure of IcsA passenger domain to the bacterial surface.

Comparison of *icsA*Arg564Ala, and *clsA* mutants revealed similar phenotypes involving IcsA localization and plaque formation. We determined that, independent of outer membrane transport; polar cardiolipin directs the IcsA cPT domain via a direct interaction with Arg564. We propose that outer membrane cardiolipin directs IcsA to the bacterial pole by directly interacting with the cPT domain. Once at the bacterial pole, the IcsA beta-barrel is inserted into the bacterial membrane followed by auto-transport of the

passenger domain to the bacterial surface (Figure 33). In the absence of cardiolipin, the passenger domain is still able to interact with outer membrane phospholipid for membrane insertion and auto-transport; however, it is not attracted to the bacterial pole, so localization is circumferential.

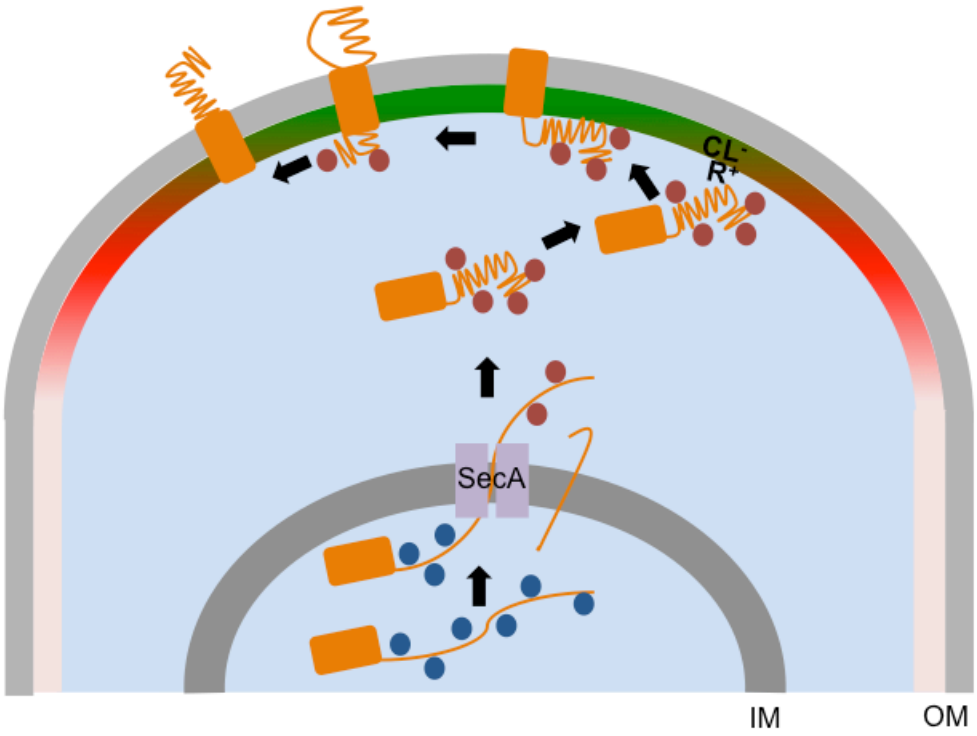

Figure 33. Model for cardiolipin directing polar IcsA localization.

IcsA is transcribed in the cytoplasm and held in a non-folded conformation by cytoplasmic chaperone proteins Skp and DnaK (blue filled circles). The signal peptide sequence of IcsA directs it to SecA for translocation across the inner membrane and subsequent cleavage of signal sequence. Upon periplasmic entry, IcsA begins to fold with the help of periplasmic chaperon proteins DegP/SurA/Skp (red filled circles). Arg546 directs interaction with the bacterial pole by targeting IcsA to cardiolipin (green region). Interaction with the outer membrane directs insertion of the IcsA beta-barrel into the membrane, followed by transport of the IcsA auto-transport domain. The N-WASP domain is now exposed at the bacterial pole to direct actin polymerization.

References

Adler, B., Sasakawa, C., Tobe, T., Makino, S., Komatsu, K. & Yoshikawa, M. (1989). A dual transcriptional activation system for the 230 kb plasmid genes coding for virulence-associated antigens of *Shigella flexneri*. *Mol Microbiology* **3**, 627–635.

Agaisse, H. (2016). Molecular and Cellular Mechanisms of *Shigella flexneri* Dissemination. *Front Cell Infect Microbiol* **6**, 29. Frontiers.

Allaoui, A., Sansonetti, P. J., Ménard, R., Barzu, S., Mounier, J., Phalipon, A. & Parsot, C. (1995). MxiG, a membrane protein required for secretion of *Shigella spp*. Ipa invasins: involvement in entry into epithelial cells and in intercellular dissemination. *Mol Microbiology* **17**, 461–470.

Allaoui, A., Sansonetti, P. J. & Parsot, C. (1992). MxiJ, a lipoprotein involved in secretion of *Shigella* Ipa invasins, is homologous to YscJ, a secretion factor of the Yersinia Yop proteins. *J Bacteriol* **174**, 7661–7669.

Allaoui, A., Sansonetti, P. J. & Parsot, C. (1993). MxiD, an outer membrane protein necessary for the secretion of the *Shigella flexneri* lpa invasins. *Mol Microbiology* **7**, 59–68.

Ambrosi, C., Pompili, M., Scribano, D., Zagaglia, C., Ripa, S. & Nicoletti, M. (2012). Outer membrane protein A (OmpA): a new player in *Shigella flexneri* protrusion formation and inter-cellular spreading. *PLoS One* **7**, e49625.

Andrews, G. P., Hromockyj, A. E., Coker, C. & Maurelli, A. T. (1991). Two novel virulence loci, mxiA and mxiB, in *Shigella flexneri* 2a facilitate excretion of invasion plasmid antigens. *Infect Immun* **59**, 1997–2005.

Ashkenazi, S., Levy, I., Kazaronovski, V. & Samra, Z. (2003). Growing antimicrobial resistance of *Shigella* isolates. *J Antimicrob Chemother* **51**, 427–429.

Baba, T., Ara, T., Hasegawa, M., Takai, Y., Okumura, Y., Baba, M., Datsenko, K. A., Tomita, M., Wanner, B. L. & Mori, H. (2006). Construction of *Escherichia coli* K-12 in-frame, single-gene knockout mutants: the Keio collection. *Mol Syst Biol* **2**, 2006.0008.

Bardhan, P., Faruque, A. S. G., Naheed, A. & Sack, D. A. (2010). Decrease in shigellosis-related deaths without *Shigella spp*.-specific interventions, Asia. *Emerging Infect Dis* **16**, 1718–1723.

Bernardini, M. L., Mounier, J., d'Hauteville, H., Coquis-Rondon, M. & Sansonetti, P. J. (1989). Identification of icsA, a plasmid locus of *Shigella flexneri* that governs bacterial intra- and intercellular spread through interaction with F-actin. *Proc Natl Acad Sci USA* **86**, 3867–3871.

Besingi, R. N. & Clark, P. L. (2015). Extracellular protease digestion to evaluate membrane protein cell surface localization. *Nat Protocols* **10**, 2074–2080.

Bhattacharya, S. K., Sarkar, K., Balakrish Nair, G., Faruque, A. S. G. & Sack, D. A. (2003). Multidrug-resistant *Shigella dysenteriae* type 1 in south Asia. *Lancet Infect Dis* **3**, 755.

Bligh, E. G. & Dyer, W. J. (1959). A rapid method of total lipid extraction and purification. *Can J Biochem Physiol* **37**, 911–917.

Brahmbhatt, H. N., Lindberg, A. A. & Timmis, K. N. (1992). *Shigella* lipopolysaccharide: structure, genetics, and vaccine development. *Curr Top Microbiol Immunol* **180**, 45–64.

Brandon, L. D. & Goldberg, M. B. (2001). Periplasmic transit and disulfide bond formation of the autotransported *Shigella* protein IcsA. *J Bacteriol* **183**, 951–958.

Brandon, L. D., Goehring, N., Janakiraman, A., Yan, A. W., Wu, T., Beckwith, J. & Goldberg, M. B. (2003). IcsA, a polarly localized autotransporter with an atypical signal peptide, uses the Sec apparatus for secretion, although the Sec apparatus is circumferentially distributed. *Mol Microbiology* **50**, 45–60.

Braun, V. (1975). Covalent lipoprotein from the outer membrane of *Escherichia coli*. *Biochim Biophys Acta* **415**, 335–377.

Brotcke Zumsteg, A., Goosmann, C., Brinkmann, V., Morona, R. & Zychlinsky, A. (2014). IcsA is a *Shigella flexneri* adhesin regulated by the type III secretion system and required for pathogenesis. *Cell Host Microbe* **15**, 435–445.

Buskirk, S. W. & Lafontaine, E. R. (2014). *Moraxella catarrhali*s expresses a cardiolipin synthase that impacts adherence to human epithelial cells. *J Bacteriol* **196**, 107–120.

Campbell-Valois, F.-X., Schnupf, P., Nigro, G., Sachse, M., Sansonetti, P. J. & Parsot, C. (2014). A fluorescent reporter reveals on/off regulation of the *Shigella* type III secretion apparatus during entry and cell-to-cell spread. *Cell Host Microbe* **15**, 177–189.

Carpenter, C. D., Cooley, B. J., Needham, B. D., Fisher, C. R., Trent, M. S., Gordon, V. & Payne, S. M. (2014). The Vps/VacJ ABC transporter is required for intercellular spread of *Shigella flexneri*. *Infect Immun* **82**, 660–669.

Carpenter, C. & Payne, S. M. (2014). Regulation of iron transport systems in *Enterobacteriaceae* in response to oxygen and iron availability. *J Inorg Biochem* **133**, 110–117.

Charles, M., Perez, M., Kobil, J. H. & Goldberg, M. B. (2001). Polar targeting of *Shigella virulence* factor IcsA in *Enterobacteriacae* and *Vibrio*. *Proc Natl Acad Sci USA* **98**, 9871–9876.

Cherepanov, P. P. & Wackernagel, W. (1995). Gene disruption in *Escherichia coli*: TcR and KmR cassettes with the option of Flp-catalyzed excision of the antibiotic-resistance determinant. *Gene* **158**, 9–14.

Clifton, L. A., Skoda, M. W. A., Daulton, E. L., Hughes, A. V., Le Brun, A. P., Lakey, J. H. & Holt, S. A. (2013). Asymmetric phospholipid: lipopolysaccharide bilayers; a Gram-negative bacterial outer membrane mimic. *J R Soc Interface* **10**, 20130810–20130810.

Dalebroux, Z. D., Edrozo, M. B., Pfuetzner, R. A., Ressl, S., Kulasekara, B. R., Blanc, M.-P. & Miller, S. I. (2015). Delivery of cardiolipins to the *Salmonella* outer membrane is necessary for survival within host tissues and virulence. *Cell Host Microbe* **17**, 441–451.

Dalebroux, Z. D., Matamouros, S., Whittington, D., Bishop, R. E. & Miller, S. I. (2014). PhoPQ regulates acidic glycerophospholipid content of the Salmonella Typhimurium outer membrane. *Proc Natl Acad Sci USA* **111**, 1963–1968.

Datsenko, K. A. & Wanner, B. L. (2000). One-step inactivation of chromosomal genes in *Escherichia coli* K-12 using PCR products. *Proc Natl Acad Sci USA* **97**, 6640–6645.

De Lay, N. R. & Cronan, J. E. (2008). Genetic interaction between the *Escherichia coli* AcpT phosphopantetheinyl transferase and the YejM inner membrane protein. *Genetics* **178**, 1327–1337.

Doyle, M. T., Grabowicz, M., May, K. L. & Morona, R. (2015a). Lipopolysaccharide surface structure does not influence IcsA polarity. *FEMS Microbiol Lett* **362**, fnv042.

Doyle, M. T., Grabowicz, M. & Morona, R. (2015b). A small conserved motif supports polarity augmentation of *Shigella flexneri* IcsA. *Microbiology* **161**, 2087–2097.

Doyle, M. T., Tran, E. N. H. & Morona, R. (2015c). The passenger-associated transport repeat promotes virulence factor secretion efficiency and delineates a distinct autotransporter subtype. *Mol Microbiol* **97**, 315–329.

Dragoi, A.-M. & Agaisse, H. (2014). The serine/threonine kinase STK11 promotes *Shigella flexneri* dissemination through establishment of cell-cell contacts competent for tyrosine kinase signaling. *Infect Immun* **82**, 4447–4457.

Dragoi, A.-M. & Agaisse, H. (2015). The class II phosphatidylinositol 3-phosphate kinase PIK3C2A promotes *Shigella flexneri* dissemination through formation of vacuole-like protrusions. *Infect Immun* **83**, 1695–1704.

Duncan, A. L., Robinson, A. J. & Walker, J. E. (2016). Cardiolipin binds selectively but transiently to conserved lysine residues in the rotor of metazoan ATP synthases. *Proc Natl Acad Sci USA* **113**, 8687–8692.

DuPont, H. L., Levine, M. M., Hornick, R. B. & Formal, S. B. (1989). Inoculum size in shigellosis and implications for expected mode of transmission. *J Infect Dis* **159**, 1126–1128.

Egile, C., Loisel, T. P., Laurent, V., Li, R., Pantaloni, D., Sansonetti, P. J. & Carlier, M. F. (1999). Activation of the CDC42 effector N-WASP by the *Shigella flexneri*

IcsA protein promotes actin nucleation by Arp2/3 complex and bacterial actin-based motility. *J Cell Biol* **146**, 1319–1332.

Fukuda, I., Suzuki, T., Munakata, H., Hayashi, N., Katayama, E., Yoshikawa, M. & Sasakawa, C. (1995). Cleavage of *Shigella* surface protein VirG occurs at a specific site, but the secretion is not essential for intracellular spreading. *J Bacteriol* **177**, 1719–1726.

Giles, D. K., Hankins, J. V., Guan, Z. & Trent, M. S. (2011). Remodelling of the *Vibrio cholerae* membrane by incorporation of exogenous fatty acids from host and aquatic environments. *Mol Microbiol* **79**, 716–728.

Goldberg, M. B., Bârzu, O., Parsot, C. & Sansonetti, P. J. (1993). Unipolar localization and ATPase activity of IcsA, a *Shigella flexneri* protein involved in intracellular movement. *J Bacteriol* **175**, 2189–2196.

Goldberg, M. B. & Theriot, J. A. (1995). *Shigella flexneri* surface protein IcsA is sufficient to direct actin-based motility. *Proc Natl Acad Sci USA* **92**, 6572–6576.

Goldberg, M. B., Theriot, J. A. & Sansonetti, P. J. (1994). Regulation of surface presentation of IcsA, a *Shigella* protein essential to intracellular movement and spread, is growth phase dependent. *Infect Immun* **62**, 5664–5668.

Gray, A. N., Li, Z., Henderson-Frost, J. & Goldberg, M. B. (2014). Biogenesis of YidC cytoplasmic membrane substrates is required for positioning of autotransporter IcsA at future poles. *J Bacteriol* **196**, 624–632.

Guo, D. & Tropp, B. E. (2000). A second *Escherichia coli* protein with CL synthase activity. *Biochim Biophys Acta* **1483**, 263–274.

Hale, T. L. & Formal, S. B. (1981). Protein synthesis in HeLa or Henle 407 cells infected with *Shigella dysenteriae* 1, *Shigella flexneri* 2a, or *Salmonella typhimurium* W118. *Infect Immun* **32**, 137–144.

Hankins, J. V., Madsen, J. A., Giles, D. K., Brodbelt, J. S. & Trent, M. S. (2012). Amino acid addition to *Vibrio cholerae* LPS establishes a link between surface remodeling in gram-positive and gram-negative bacteria. *Proc Natl Acad Sci USA* **109**, 8722–8727.

High, N., Mounier, J., Prévost, M. C. & Sansonetti, P. J. (1992). IpaB of *Shigella flexneri* causes entry into epithelial cells and escape from the phagocytic vacuole. *EMBO J* **11**, 1991–1999.

Hiraoka, S., Matsuzaki, H. & Shibuya, I. (1993). Active increase in cardiolipin synthesis in the stationary growth phase and its physiological significance in *Escherichia coli*. *FEBS lett* **336**, 221–224.

Hirvas, L., Nurminen, M., Helander, I. M., Vuorio, R. & Vaara, M. (1997). The lipid A biosynthesis deficiency of the *Escherichia coli* antibiotic-supersensitive mutant LH530 is suppressed by a novel locus, ORF195. *Microbiology* **143 (Pt 1)**, 73–81.

Hong, M. & Payne, S. M. (1997). Effect of mutations in *Shigella flexneri* chromosomal and plasmid-encoded lipopolysaccharide genes on invasion and serum resistance. *Mol Microbiol* **24**, 779–791.

Hsieh, C. W., Lin, T. Y., Lai, H. M., Lin, C. C., Hsieh, T. S. & Shih, Y. L. (2010). Direct MinE-membrane interaction contributes to the proper localization of MinDE in *E. coli*. *Mol Microbiol* **75**, 499–512.

Janakiraman, A., Fixen, K. R., Gray, A. N., Niki, H. & Goldberg, M. B. (2009). A genome-scale proteomic screen identifies a role for DnaK in chaperoning of polar autotransporters in *Shigella*. *J Bacteriol* **191**, 6300–6311.

Kamio, Y. & Nikaido, H. (1976). Outer membrane of *Salmonella typhimurium*: accessibility of phospholipid head groups to phospholipase c and cyanogen bromide activated dextran in the external medium. *Biochemistry* **15**, 2561–2570.

Kenne, L., Lindberg, B., Petersson, K., Katzenellenbogen, E. & Romanowska, E. (1978). Structural studies of *Shigella flexneri* O-antigens. *Eur J Biochem* **91**, 279–284.

Koprivnjak, T., Zhang, D., Ernst, C. M., Peschel, A., Nauseef, W. M. & Weiss, J. P. (2011). Characterization of *Staphylococcus aureus* cardiolipin synthases 1 and 2 and their contribution to accumulation of cardiolipin in stationary phase and within phagocytes. *J Bacteriol* **193**, 4134–4142.

Kotloff, K. L., Winickoff, J. P., Ivanoff, B., Clemens, J. D., Swerdlow, D. L., Sansonetti, P. J., Adak, G. K. & Levine, M. M. (1999). Global burden of *Shigella* infections: implications for vaccine development and implementation of control strategies. *Bull World Health Organ* **77**, 651–666.

Kotloff, K. L., Nataro, J. P., Blackwelder, W. C., Nasrin, D., Farag, T. H., Panchalingam, S., Wu, Y., Sow, S. O., Sur, D. & other authors. (2013). Burden and aetiology of diarrhoeal disease in infants and young children in developing countries (the Global Enteric Multicenter Study, GEMS): a prospective, case-control study. *Lancet* **382**, 209–222.

Kuehl, C. J., Dragoi, A.-M. & Agaisse, H. (2014). The *Shigella flexn*eri type 3 secretion system is required for tyrosine kinase-dependent protrusion resolution, and vacuole escape during bacterial dissemination. *PLoS One* **9**, e112738

Kühnel, K. & Diezmann, D. (2011). Crystal structure of the autochaperone region from the Shigella flexneri autotransporter IcsA. *J Bacteriol* **193**, 2042–2045.

Labrec, E. H., Schneider, H., Magnani, T. J. & Formal, S. B. (1964). Epithelial Cell Penetration as an Essential Step in the Pathogenesis of Bacillary Dysentery. *J Bacteriol* **88**, 1503–1518.

Laemmli, U. K. (1970). Cleavage of structural proteins during the assembly of the head of bacteriophage T4. *Nature* **227**, 680–685.

Lan, R. & Reeves, P. R. (2002). *Escherichia coli* in disguise: molecular origins of *Shigella*. *Microbes Infect* **4**, 1125–1132.

Leupold, S., Büsing, P., Mas, P. J., Hart, D. J. & Scrima, A. (2017). Structural insights into the architecture of the *Shigella flexneri* virulence factor IcsA/VirG and motifs involved in polar distribution and secretion. *J Struct Biol* **198**, 19–27.

Leyton, D. L., Rossiter, A. E. & Henderson, I. R. (2012). From self sufficiency to dependence: mechanisms and factors important for autotransporter biogenesis. *Nat Rev Microbiol* **10**, 213–225.

Lin, T. Y., Santos, T. M. A., Kontur, W. S., Donohue, T. J. & Weibel, D. B. (2015). A Cardiolipin-Deficient Mutant of *Rhodobacter sphaeroides* Has an Altered Cell Shape and Is Impaired in Biofilm Formation. *J Bacteriol* **197**, 3446–3455

López, C. S., Alice, A. F., Heras, H., Rivas, E. A. & Sánchez-Rivas, C. (2006). Role of anionic phospholipids in the adaptation of *Bacillus subtilis* to high salinity. *Microbiology* **152**, 605–616.

Makino, S., Sasakawa, C., Kamata, K., Kurata, T. & Yoshikawa, M. (1986). A genetic determinant required for continuous reinfection of adjacent cells on large plasmid in *S. flexneri* 2a. *Cell* **46**, 551–555.

Malinverni, J. C. & Silhavy, T. J. (2009). An ABC transport system that maintains lipid asymmetry in the gram-negative outer membrane. *Proc Natl Acad Sci USA* **106**, 8009–8014.

Mavris, M., Page, A.-L., Tournebize, R., Demers, B. & Parsot, C. (2002). Regulation of transcription by the activity of the *Shigella flexneri t*ype III secretion apparatus. *Mol Microbiol* **43**, 1543–1553.

May, K. L. & Morona, R. (2008). Mutagenesis of the *Shigella flexneri* autotransporter IcsA reveals novel functional regions involved in IcsA biogenesis and recruitment of host neural Wiscott-Aldrich syndrome protein. *J Bacteriol* **190**, 4666–4676.

Mileykovskaya, E., Zhang, M. & Dowhan, W. (2005). Cardiolipin in energy transducing membranes. *Biochemistry* **70**, 154–158.

Morona, R., Van den Bosch, L. & Manning, P. A. (1995). Molecular, genetic, and topological characterization of O-antigen chain length regulation in *Shigella flexneri*. *J Bacteriol* **177**, 1059–1068.

Morona, R. & Van Den Bosch, L. (2003). Lipopolysaccharide O antigen chains mask IcsA (VirG) in *Shigella flexneri*. *FEMS Microbiol Lett* **221**, 173–180.

Musher, D. M. & Musher, B. L. (2004). Contagious acute gastrointestinal infections. *N Engl J Med* **351**, 2417–2427.

Needham, B. D. & Trent, M. S. (2013). Fortifying the barrier: the impact of lipid A remodelling on bacterial pathogenesis. **11**, 467–481.

Oaks, E. V., Wingfield, M. E. & Formal, S. B. (1985). Plaque formation by virulent *Shigella flexneri*. *Infect Immun* **48**, 124–129.

Oliver, P. M., Crooks, J. A., Leidl, M., Yoon, E. J., Saghatelian, A. & Weibel, D. B. (2014). Localization of anionic phospholipids in *Escherichia coli* cells. *J Bacteriol* **196**, 3386–3398.

Paciello, I., Silipo, A., Lembo-Fazio, L., Curcurù, L., Zumsteg, A., Noël, G., Ciancarella, V., Sturiale, L., Molinaro, A. & Bernardini, M. L. (2013). Intracellular *Shigella* remodels its LPS to dampen the innate immune recognition and evade inflammasome activation. *Proc Natl Acad Sci USA* **110**, E4345–54.

Page, A. L., Ohayon, H., Sansonetti, P. J. & Parsot, C. (1999). The secreted IpaB and IpaC invasins and their cytoplasmic chaperone IpgC are required for intercellular dissemination of *Shigella flexneri*. *Cellular Microbiology* **1**, 183–193.

Pangborn, M. C. (1945). A simplified preparation of cardiolipin, with note on purification of lecithin for serologic use. *J Biol Chem* **161**, 71–82.

Payne, S. M. & Finkelstein, R. A. (1977). Detection and differentiation of iron-responsive avirulent mutants on Congo red agar. *Infect Immun* **18**, 94–98.

Philpott, D. J., Edgeworth, J. D. & Sansonetti, P. J. (2000). The pathogenesis of *Shigella flexneri* infection: lessons from in vitro and in vivo studies. *Philos Trans R Soc Lond B Biol Sci* **355**, 575–586.

Pluschke, G., Hirota, Y. & Overath, P. (1978). Function of phospholipids in *Escherichia coli*. Characterization of a mutant deficient in cardiolipin synthesis. *J Biol Chem* **253**, 5048–5055.

Pope, L. M., Reed, K. E. & Payne, S. M. (1995). Increased protein secretion and adherence to HeLa cells by *Shigella spp*. following growth in the presence of bile salts. *Infect and Immun* **63**, 3642–3648.

Purdy, G. E., Fisher, C. R. & Payne, S. M. (2007). IcsA surface presentation in *Shigella flexneri* requires the periplasmic chaperones DegP, Skp, and SurA. *J Bacteriol* **189**, 5566–5573.

Purdy, G. E., Hong, M. & Payne, S. M. (2002). *Shigella flexneri* DegP facilitates IcsA surface expression and is required for efficient intercellular spread. *Infect Immun* **70**, 6355–6364.

Raetz, C. R. H., Reynolds, C. M., Trent, M. S. & Bishop, R. E. (2007). Lipid A modification systems in gram-negative bacteria. *Annu Rev Biochem* **76**, 295–329.

Ram, P. K., Crump, J. A., Gupta, S. K., Miller, M. A. & Mintz, E. D. (2008). Part II. Analysis of data gaps pertaining to *Shigella* infections in low and medium human development index countries, 1984-2005. *Epidemiol Infect* **136**, 577–603.

Ramamurthi, K. S. & Losick, R. (2009). Negative membrane curvature as a cue for subcellular localization of a bacterial protein. *Proc Natl Acad Sci USA* **106**, 13541–13545.

Renner, L. D. & Weibel, D. B. (2011). Cardiolipin microdomains localize to negatively curved regions of *Escherichia coli* membranes. *Proc Natl Acad Sci USA* **108**, 6264–6269.

Renner, L. D. & Weibel, D. B. (2012). MinD and MinE interact with anionic phospholipids and regulate division plane formation in *Escherichia coli*. *J Biol Chem* **287**, 38835–38844.

Robbins, J. R., Monack, D., McCallum, S. J., Vegas, A., Pham, E., Goldberg, M. B. & Theriot, J. A. (2001). The making of a gradient: IcsA (VirG) polarity in *Shigella flexneri*. *Mol Microbiol* **41**, 861–872.

Romantsov, T., Guan, Z. & Wood, J. M. (2009). Cardiolipin and the osmotic stress responses of bacteria. *Biochim Biophys Acta* **1788**, 2092–2100.

Rossi, R. M., Yum, L., Agaisse, H. & Payne, S. M. (2017). Cardiolipin Synthesis and Outer Membrane Localization Are Required for *Shigella flexneri* Virulence. *mBio* **8**, e01199–17.

Sandlin, R. C., Lampel, K. A., Keasler, S. P., Goldberg, M. B., Stolzer, A. L. & Maurelli, A. T. (1995). Avirulence of rough mutants of *Shigella flexneri*: requirement of O antigen for correct unipolar localization of IcsA in the bacterial outer membrane. *Infect Immun* **63**, 229–237.

Sansonetti, P. J. (2001). Rupture, invasion and inflammatory destruction of the intestinal barrier by *Shigella*, making sense of prokaryote-eukaryote cross-talks. *FEMS Microbiol Rev* **25**, 3–14.

Sansonetti, P. J., Arondel, J., Cantey, J. R., Prévost, M. C. & Huerre, M. (1996). Infection of rabbit Peyer's patches by Shigella flexneri: effect of adhesive or invasive bacterial phenotypes on follicle-associated epithelium. *Infect Immun* **64**, 2752–2764.

Sansonetti, P. J., Kopecko, D. J. & Formal, S. B. (1982). Involvement of a plasmid in the invasive ability of *Shigella flexneri*. *Infect Immun* **35**, 852–860.

Sansonetti, P. J., Ryter, A., Clerc, P., Maurelli, A. T. & Mounier, J. (1986). Multiplication of *Shigella flexneri* within HeLa cells: lysis of the phagocytic vacuole and plasmid-mediated contact hemolysis. *Infect Immun* **51**, 461–469.

Santapaola, D., Del Chierico, F., Petrucca, A., Uzzau, S., Casalino, M., Colonna, B., Sessa, R., Berlutti, F. & Nicoletti, M. (2006). Apyrase, the product of the virulence plasmid-encoded phoN2 (apy) gene of *Shigella flexneri*, is necessary for proper unipolar IcsA localization and for efficient intercellular spread. *J Bacteriol* **188**, 1620–1627.

Schenkel, L. C. & Bakovic, M. (2014). Formation and regulation of mitochondrial membranes. *Int J Cell Biol* **2014**, 709828–13.

Schneider, C. A., Rasband, W. S. & Eliceiri, K. W. (2012). NIH Image to ImageJ: 25 years of image analysis. *Nat Methods* **9**, 671–675.

Schroeder, G. N. & Hilbi, H. (2008). Molecular pathogenesis of *Shigella spp.*: controlling host cell signaling, invasion, and death by type III secretion. *Clin Microbiol Rev* **21**, 134–156.

Schwechheimer, C. & Kuehn, M. J. (2015). Outer-membrane vesicles from Gram-negative bacteria: biogenesis and functions. *Nat Rev Microbiol* **13**, 605–619.

Scribano, D., Damico, R., Ambrosi, C., Superti, F., Marazzato, M., Conte, M. P., Longhi, C., Palamara, A. T., Zagaglia, C. & Nicoletti, M. (2016). The *Shigella flexneri* OmpA amino acid residues 188EVQ190 are essential for the interaction with the virulence factor PhoN2. *Biochem Biophys Rep* **8**, 168–173.

Scribano, D., Petrucca, A., Pompili, M., Ambrosi, C., Bruni, E., Zagaglia, C., Prosseda, G., Nencioni, L., Casalino, M. & other authors. **(2014).** Polar localization of PhoN2, a periplasmic virulence-associated factor of Shigella flexneri, is required for proper IcsA exposition at the old bacterial pole. *PLoS One* **9**, e90230.

Shere, K. D., Sallustio, S., Manessis, A., D'Aversa, T. G. & Goldberg, M. B. (1997). Disruption of IcsP, the major *Shigella* protease that cleaves IcsA, accelerates actin-based motility. *Mol Microbiol* **25**, 451–462.

Silhavy, T. J., Kahne, D. & Walker, S. (2010). The bacterial cell envelope. *Cold Spring Harb Perspect Biol* **2**, a000414–a000414.

Simmons, D. A. & Romanowska, E. (1987). Structure and biology of *Shigella flexneri* O antigens. *J Med Microbiol* **23**, 289–302.

Subramani, S., Perdreau-Dahl, H. & Morth, J. P. (2016). The magnesium transporter A is activated by cardiolipin and is highly sensitive to free magnesium in vitro. *Elife* **5**, 727.

Suzuki, T., Lett, M. C. & Sasakawa, C. (1995). Extracellular transport of VirG protein in *Shigella*. *J Biol Chem* **270**, 30874–30880.

Suzuki, T., Mimuro, H., Suetsugu, S., Miki, H., Takenawa, T. & Sasakawa, C. (2002). Neural Wiskott-Aldrich syndrome protein (N-WASP) is the specific ligand for *Shigella* VirG among the WASP family and determines the host cell type allowing actin-based spreading. *Cellul Microbiol* **4**, 223–233.

Tan, B. K., Bogdanov, M., Zhao, J., Dowhan, W., Raetz, C. R. H. & Guan, Z. (2012). Discovery of a cardiolipin synthase utilizing phosphatidylethanolamine and phosphatidylglycerol as substrates. *Proc Natl Acad Sci USA* **109**, 16504–16509.

Teh, M. Y. & Morona, R. (2013). Identification of *Shigella flexneri* IcsA residues affecting interaction with N-WASP, and evidence for IcsA-IcsA co-operative interaction. *PLoS One* **8**, e55152.

Thapar, N. & Sanderson, I. R. (2004). Diarrhoea in children: an interface between developing and developed countries. *Lancet* **363**, 641–653.

Thompson, C. N., Duy, P. T. & Baker, S. (2015). The Rising Dominance of *Shigella sonnei*: An Intercontinental Shift in the Etiology of Bacillary Dysentery. *PLoS Negl Trop Dis* **9**, e0003708.

Tobe, T., Nagai, S., Okada, N., Adler, B., Yoshikawa, M. & Sasakawa, C. (1991). Temperature-regulated expression of invasion genes in *Shigella flexneri* is controlled through the transcriptional activation of the virB gene on the large plasmid. *Mol Microbiol* **5**, 887–893.

Tran, E. N. H., Doyle, M. T. & Morona, R. (2013). LPS unmasking of *Shigella flexneri* reveals preferential localisation of tagged outer membrane protease IcsP to septa and new poles. *PLoS One* **8**, e70508.

Tsai, C. M. & Frasch, C. E. (1982). A sensitive silver stain for detecting lipopolysaccharides in polyacrylamide gels. *Anal Biochem* **119**, 115–119.

Venkatesan, M. M., Buysse, J. M. & Oaks, E. V. (1992). Surface presentation of *Shigella flexneri* invasion plasmid antigens requires the products of the spa locus. *J Bacteriol* **174**, 1990–2001.

Vohra, P. & Blakely, G. W. (2013). Easing the global burden of diarrhoeal disease: can synthetic biology help? *Syst Synth Biol* **7**, 73–78.

Wang, R. F. & Kushner, S. R. (1991). Construction of versatile low-copy-number vectors for cloning, sequencing and gene expression in *Escherichia coli*. *Gene* **100**, 195–199.

Waters, C. M., Lu, W., Rabinowitz, J. D. & Bassler, B. L. (2008). Quorum sensing controls biofilm formation in Vibrio cholerae through modulation of cyclic di-GMP levels and repression of vpsT. *J Bacteriol* **190**, 2527–2536.

Wei, J., Goldberg, M. B., Burland, V., Venkatesan, M. M., Deng, W., Fournier, G., Mayhew, G. F., Plunkett, G., Rose, D. J. & other authors. (2003). Complete genome sequence and comparative genomics of *Shigella flexneri* serotype 2a strain 2457T. *Infect Immun* **71**, 2775–2786.

Yankovskaya, V., Horsefield, R., Törnroth, S., Luna-Chavez, C., Miyoshi, H., Léger, C., Byrne, B., Cecchini, G. & Iwata, S. (2003). Architecture of succinate dehydrogenase and reactive oxygen species generation. *Science* **299**, 700–704.

Zhao, H. & Lappalainen, P. (2012). A simple guide to biochemical approaches for analyzing protein-lipid interactions. *Mol Biol of Cell* **23**, 2823–2830.

Zychlinsky, A., Prévost, M. C. & Sansonetti, P. J. (1992). *Shigella flexneri* induces apoptosis in infected macrophages. *Nature* **358**, 167–169.

Author Vita

Rachael Madlyn Rossi was born in Southwest Michigan, in 1990. After graduating from Waterford Mott High School, Waterford, Michigan, in 2008, she attended Michigan State University, East Lansing, Michigan. During her time at Michigan State University, she worked in the laboratory of Terence Marsh, and she received her Bachelor of Science from Michigan State University, double majoring in Microbiology and Genomics & Molecular Genetics, in May 2012. Following graduation, she worked as a research associate at Pfizer Inc., Kalamazoo, Michigan, in the Bioprocess Development Group. In August 2013, she attended the Graduate School at The University of Texas at Austin, Austin, Texas, in the laboratory of Shelley Payne. She received her Doctor of Philosophy in Microbiology from The University of Texas at Austin, in December 2017, and is currently a Postdoctoral Fellow at the University of Washington, Seattle, Washington, in the laboratory of Ferric Fang.

Address: rossirach1@gmail.com

This dissertation was typed by the author.